

GV

Measurement of Current Dependent Coherent Beam
Phenomena at the BNL VUV Storage Ring.

G. Vignola, BNL.
B. Craft, BNL. + other
S. Chattopadhyay, LBL.

December 12, 1985
Berkeley

This report describes some preliminary experimental studies of current dependent coherent beam phenomena at the BNL VUV Storage Ring, a high brightness synchrotron radiation source in the vacuum ultraviolet region. In particular we report on the observations of bunch length as a function of bunch current, parasitic mode energy loss of the beam and the longitudinal dipole and quadrupole synchrotron mode beam response (as a function of bunch current). The data provide us with information about the dependence of bunch length on current and with estimates of the resistive and reactive parts of the longitudinal beam storage ring coupling impedance of the VUV ring.

The experiments were performed during the Machine Studies Period of November 18-20, 1985 as part of a set of experimental studies, envisaged to continue till the middle of 1986. The goal of these experiments is to extract some of the generic aspects of beam dynamical behavior of low emittance, high brightness electron storage rings in the 1-2 GeV and 5-6 GeV range (popular as synchrotron radiation sources presently) in general and of the VUV and X-ray ring at BNL in particular.

Bunch Length vs. Current

Bunch lengths were measured by monitoring the light signal from single bunches (coasting in the storage ring at 744 MeV) by a fast photo-diode and observing the output electrical pulse through a fast sampling scope. The resolution (bandwidth) of the whole monitoring device was small enough to provide reasonable bunch

length data for circulating currents above 30 mA. Measurements were made for three different RF voltages ($V_{RF} = 45.5$ kV, 63.2 kV and 102.7 kV) as a function of bunch currents, upto a current of 400 mA in a single bunch. The zero intensity natural r.m.s. bunch lengths (determined by synchrotron radiation and quantum fluctuations) corresponding to the above three RF voltages seen by the beam are

$$(\sigma_e)_{\text{natural}} = 210 \text{ ps}, 176 \text{ ps} \text{ and } 137 \text{ ps} \text{ respectively.}$$

A typical longitudinal bunch profile, observed on the scope, is shown in Fig. 1. The bunch current vs. bunch length data are shown in Fig. 2 on a logarithmic scale for both axes and are summarized in Table I below. The bunch lengthening data are also

Table - I.

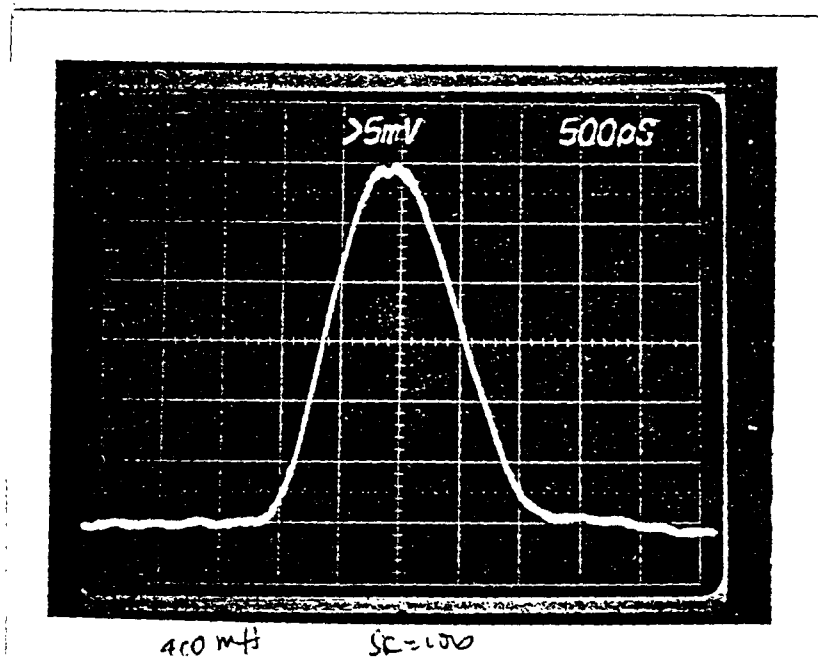
V_{RF} (kV)	σ_e (ps)	I_0 (mA)	$[\sigma_e]_{\text{nat.}}$ (ps)
45.5	$[\sigma]_{\text{nat.}} \cdot (I/I_0)^{.55}; I > I_0$	62	210
63.2	$[\sigma]_{\text{nat.}} \cdot (I/I_0)^{.55}; I > I_0$	60	176
102.7	$[\sigma]_{\text{nat.}} \cdot (I/I_0)^{.55}; I > I_0$	41	137

plotted on a linear scale in Fig. 3. The current values in Fig. 3 are those read on a TV monitor and have been corrected by a reduction factor of 10% (i.e. divided by 1.1) in obtaining the logarithmic plot in Fig. 2.

Inspection of the logarithmic plot of Fig. 2 shows the current dependence of bunch lengthening to be approximately given by:

$$\sigma_e = [\sigma_e]_{\text{nat.}} \cdot (I/I_0)^{0.55}$$

4. Pure microwave turbulent blow-up is expected to give an one-third power dependence on beam current (i.e. $\sigma_e \propto (I/I_0)^{1/3}$). However as we will see under the beam response measurements, the synchrotron tune has been observed to change with beam current. Therefore the above current dependence of bunch lengthening has to be understood as a combined effect of potential well distortion, microwave blow-up and possibly, special frequency dependence of the longitudinal impedance.



Bunch profile at $V_{RF} = 102.7$ kV, $I = 400$ mA.

Fig. 1.

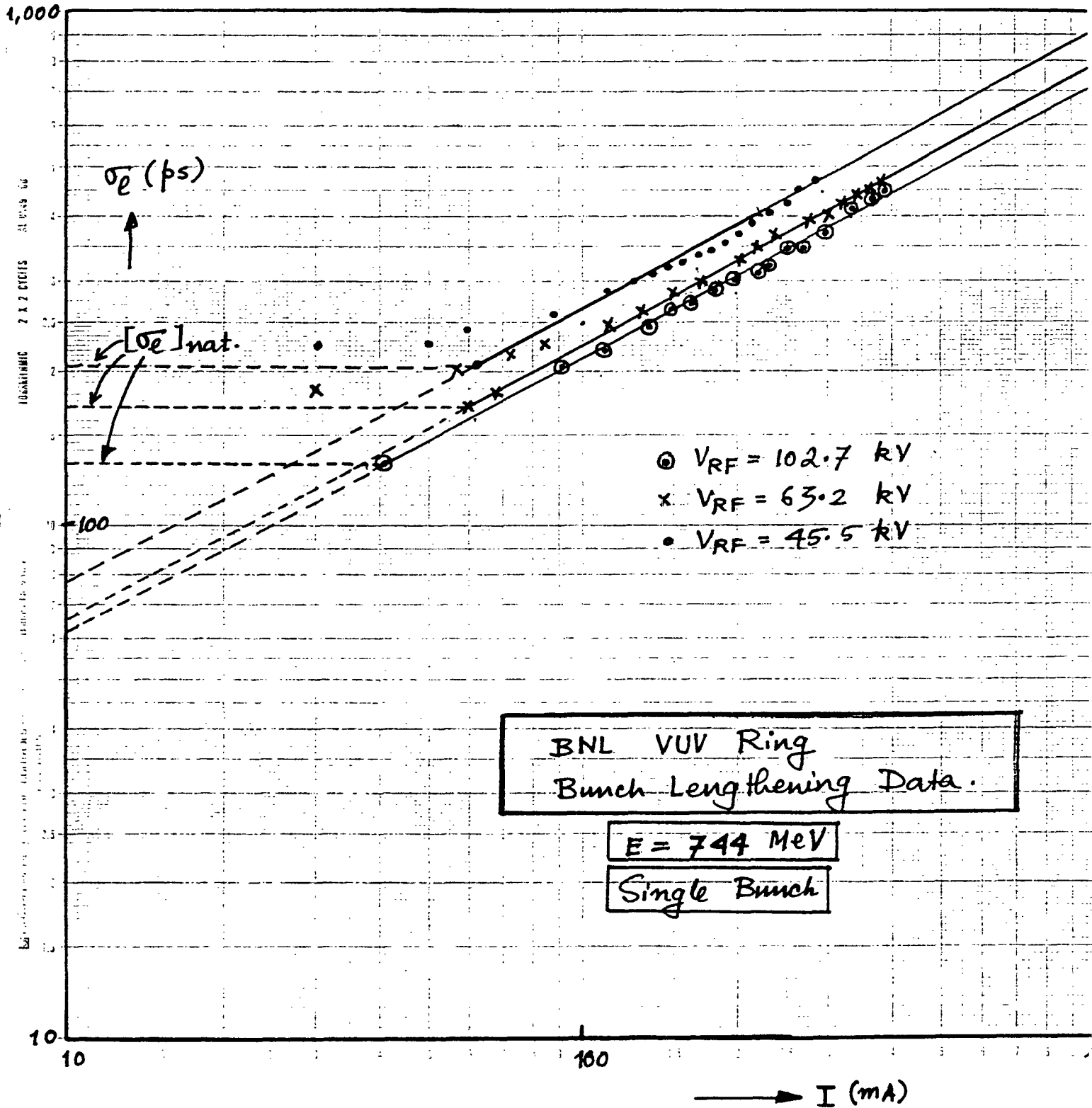


Fig. 2.

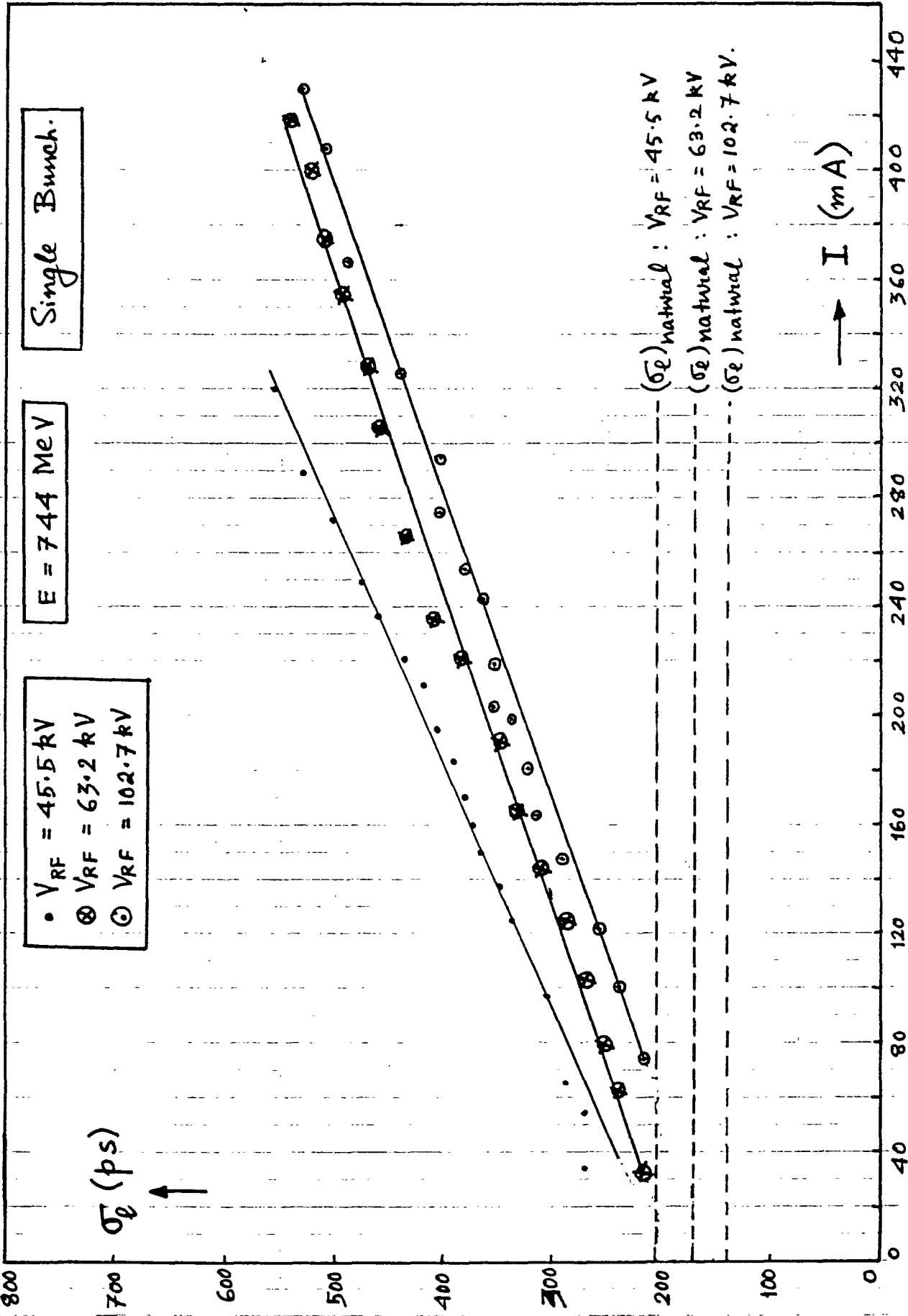


Fig. 3.

Parasitic Mode Loss Experiment.

The real resistive part of the longitudinal coupling impedance will do work on the beam or equivalently the beam will dissipate energy across the equivalent resistance of the complex impedance $Z(\omega)$. The process is usually quantified by the parasitic mode loss parameter $k_{[1]}$. For a stable stored beam, the energy loss means that the synchronous phase angle of the bunch, ϕ_s , must increase with increasing bunch current in order to compensate for the increasing loss.

We measured the parasitic mode loss parameter at the VUV ring by measuring the relative phase between the 52.885 MHz signal from the RF cavity loop and from the beam (i.e. the filtered RF component of the bunch signal from the longitudinal stripline VSUM PU) as a function of beam current. The experimental set-up is illustrated schematically in Fig. 4.

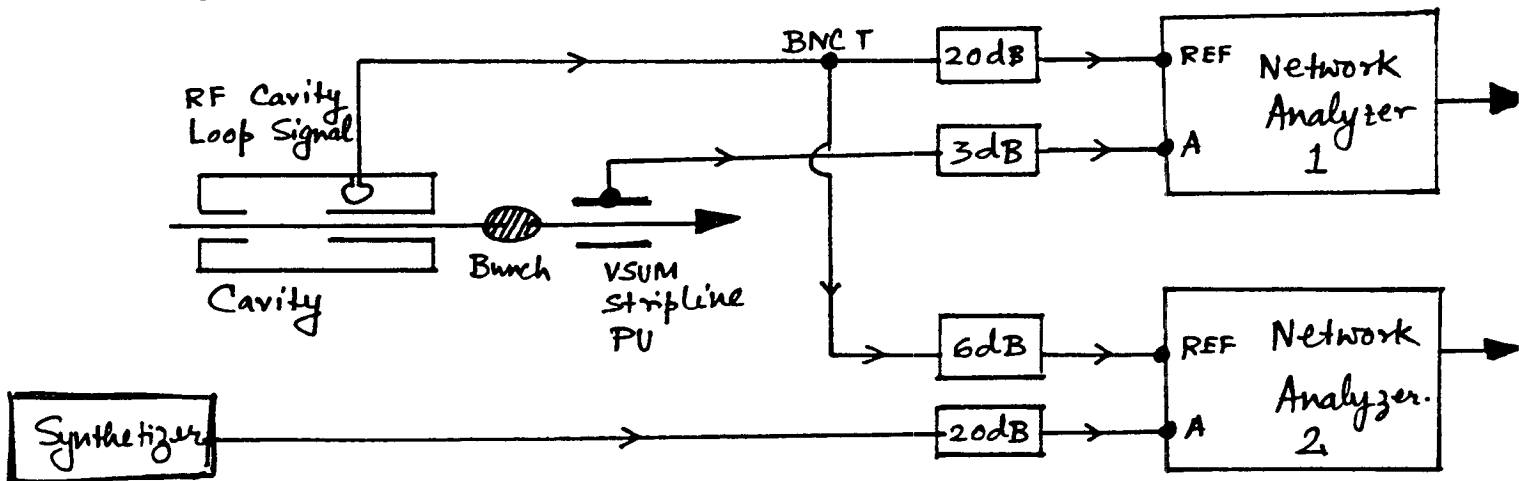


Fig. 4. Parasitic Mode Loss Experimental set-up.

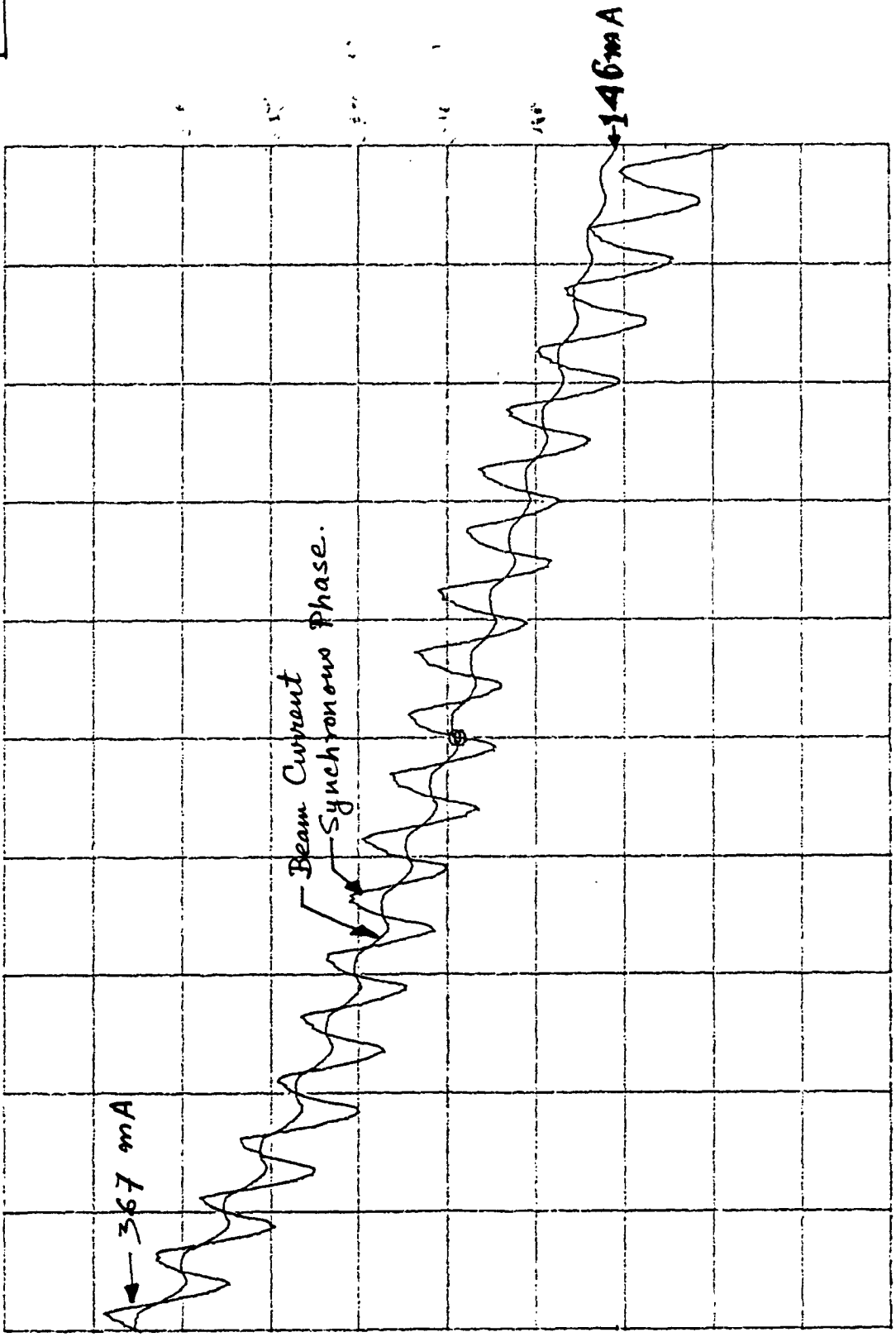
8.
Figs. 5, 6 and 7 show the bunch synchronous phase angle together with the decaying beam current as a function of time for the three different RF voltages, $V_{RF} = 102.7$ kV, 63.2 kV and 45.5 kV respectively. The slow ripple on the intensity and phase curves is a manifestation of the variation of the RF itself, as has been determined by comparing the RF loop signal directly against an external synthesizer viz. Fig. 8. These ripples are probably due to the slow temperature fluctuation in the RF temperature control loop itself.

The almost linear rise of synchronous phase with beam current are plotted in Figs. 9 and 10 for the $V_{RF} = 102.7$ kV and 45.5 kV respectively. These curves are derived from Fig. 5 and 7 respectively. The slope of these curves can be used to estimate the resistive component of the broadband impedance.

775

REF LEVEL /DIV MARKER 52 885 534.038Hz
 0.0 MAG (A/R) 2.4962
 225.30deg MARKER 52 885 534.038Hz
 PHASE (A/R) -134.776deg

V_{RF} = 102.7 kV
 E = 744 MeV



CENTER 52 885 534.038Hz SPAN 0.000Hz
 AMPTD 15.0dBm

Fig. 5

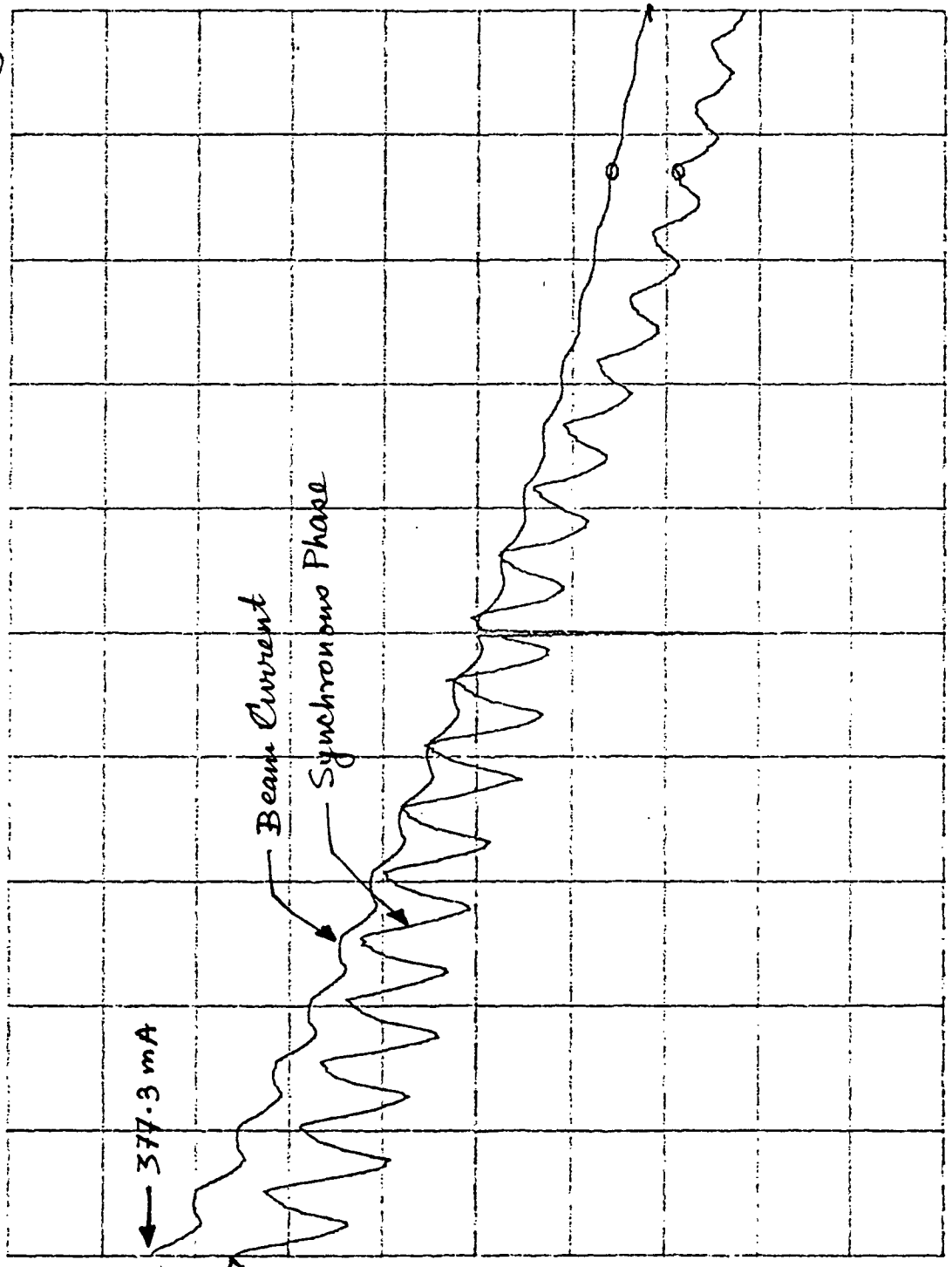
1

11/19/85
20:30

VRF = 63.2 kV

E = 744 MeV

REF LEVEL /DIV MARKER 52 885 534.038Hz
 0.0 507.81E-3 MAG (A/R) 1.8215
 225.75deg 0.500deg MARKER 52 885 534.038Hz
 PHASE (A/R) -135.310deg



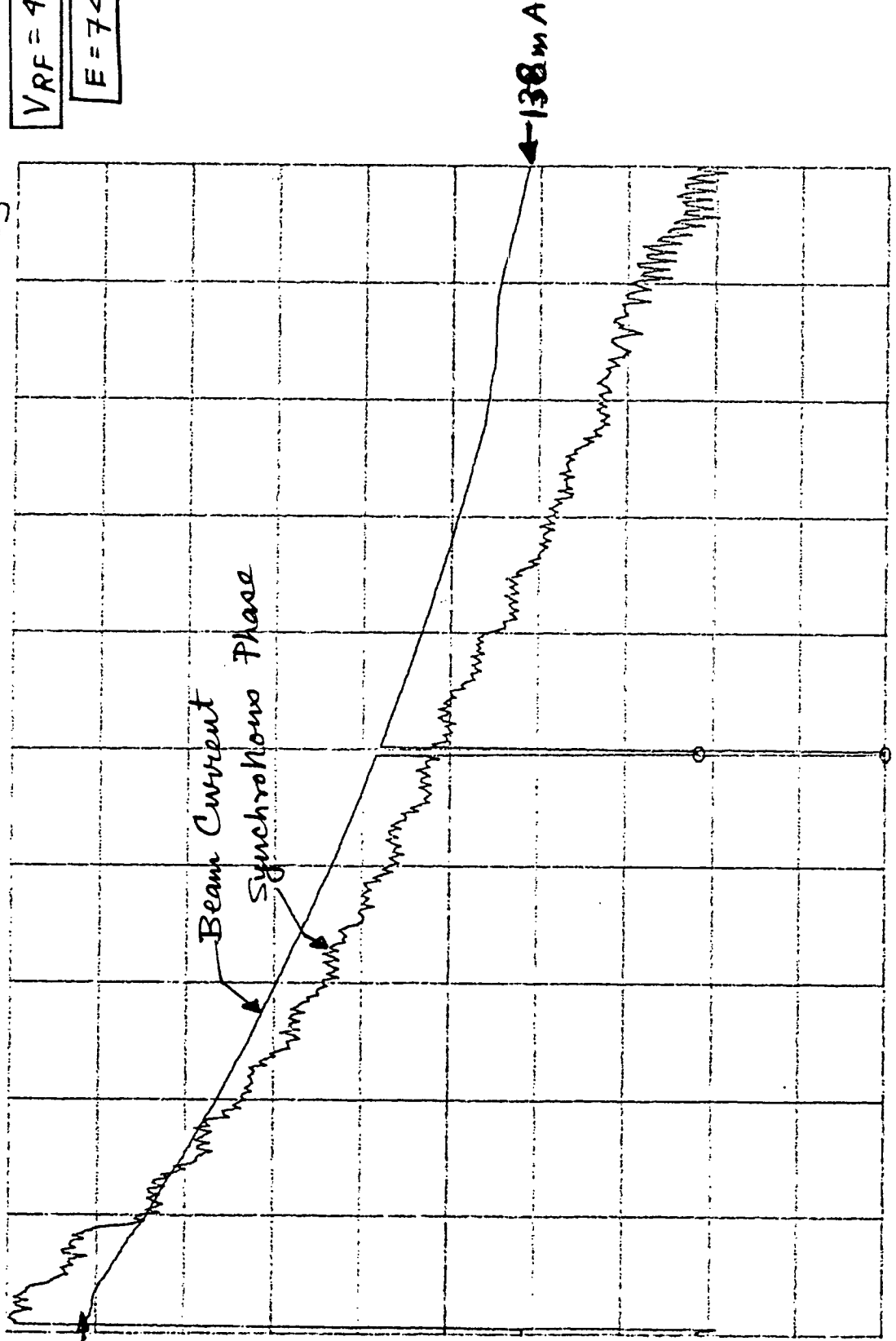
CENTER 52 885 534.038Hz SPAN 0.000Hz
 AMPTD 15.0dBm

Fig. 6

3
11/19/85
21:00 PM

$V_{RF} = 45.5 \text{ kV}$
 $E = 7.44 \text{ MeV}$

REF LEVEL /DIV MANUAL 52 885 534.038Hz
0.0 507.81E-3 MAG (A/R) 1.0935
230.55deg 0.150deg MANUAL 52 885 534.038Hz
PHASE (A/R) -137.912deg



CENTER 52 885 534.038Hz SPAN 0.000Hz
AMPTD 15.0dBm

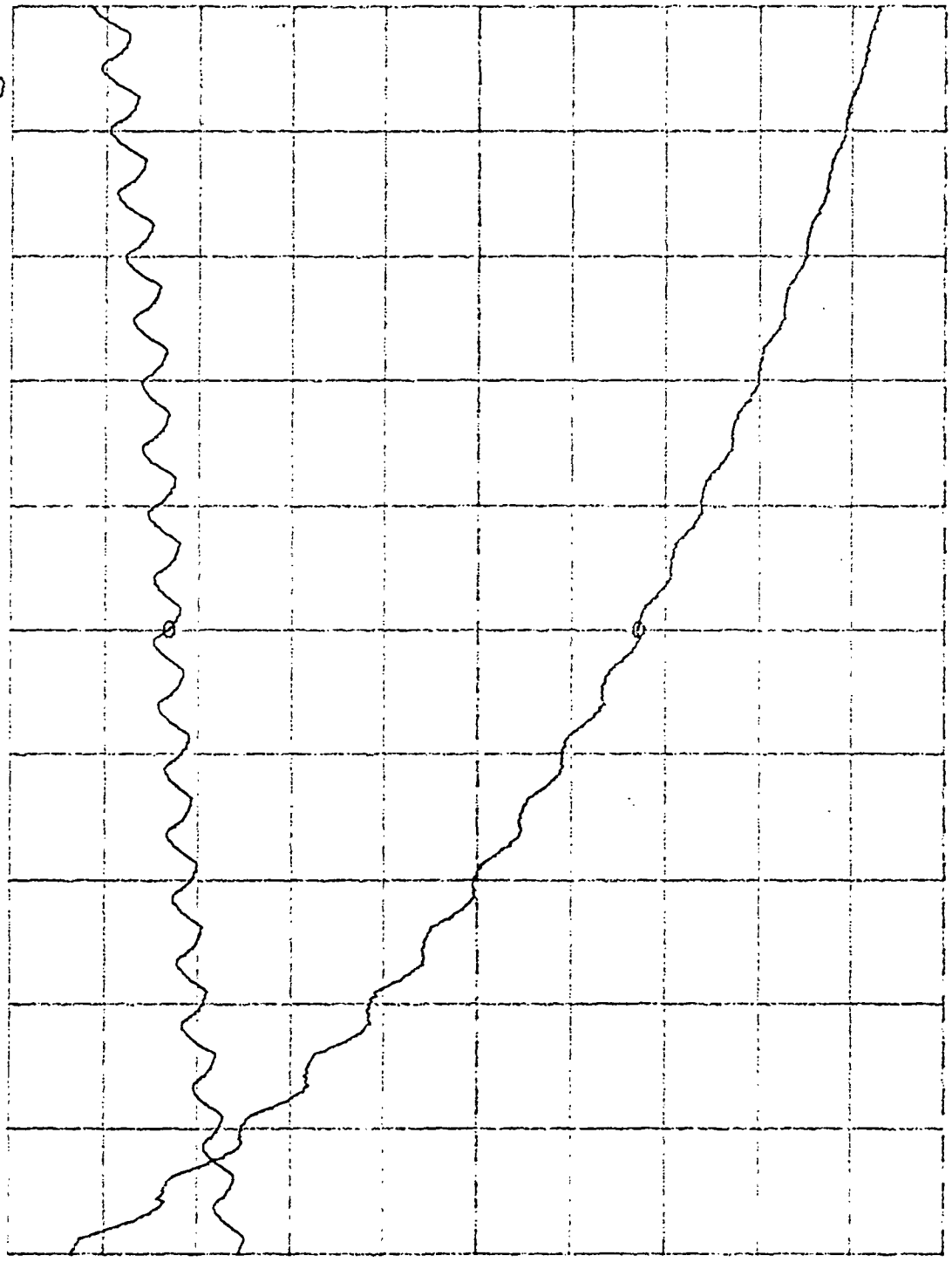
Fig. 7

#6

REF LEVEL /DIV MARKER 52 885 531.622Hz
 0.0 MAG (A/R) 3.3257
 -50.500deg MARKER 52 885 531.622Hz
 PHASE (A/R) -54.772deg

VRF = 102.7 kV

E = 744 MeV



CENTER 52 885 531.622Hz SPAN 0.000Hz
 AMPTD -10.0dBm

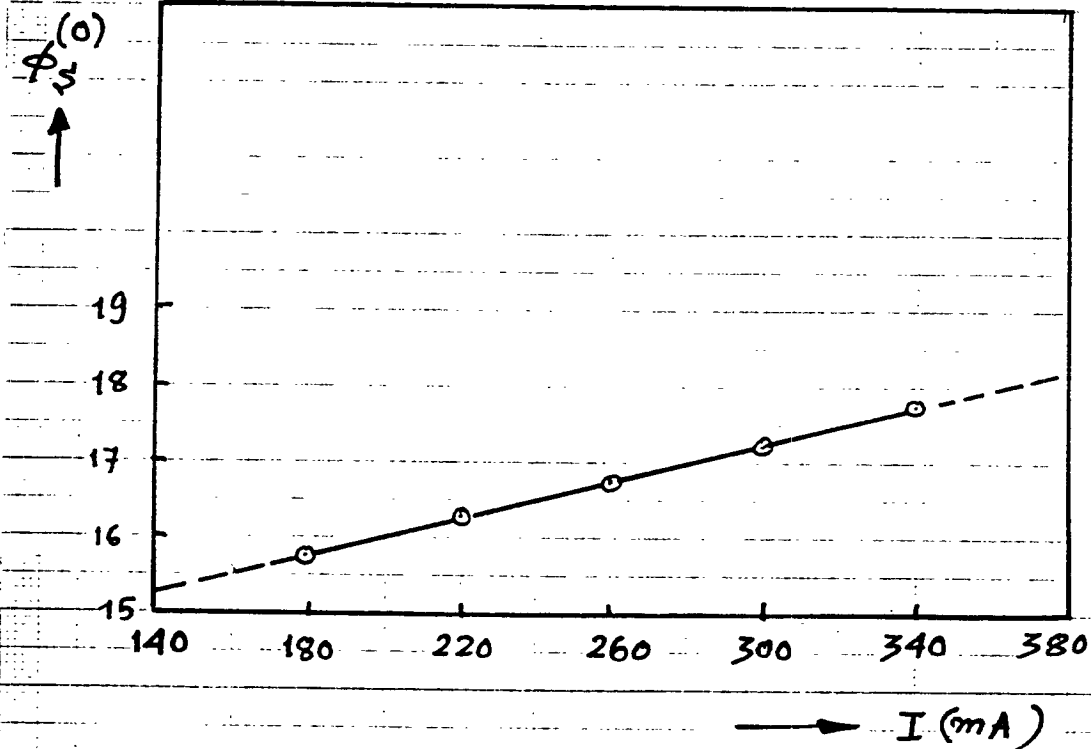
Fig. 8

Single Bunch

$$V_{RF} = 102.7 \text{ kV}$$

$$E = 744 \text{ MeV}$$

Degrees



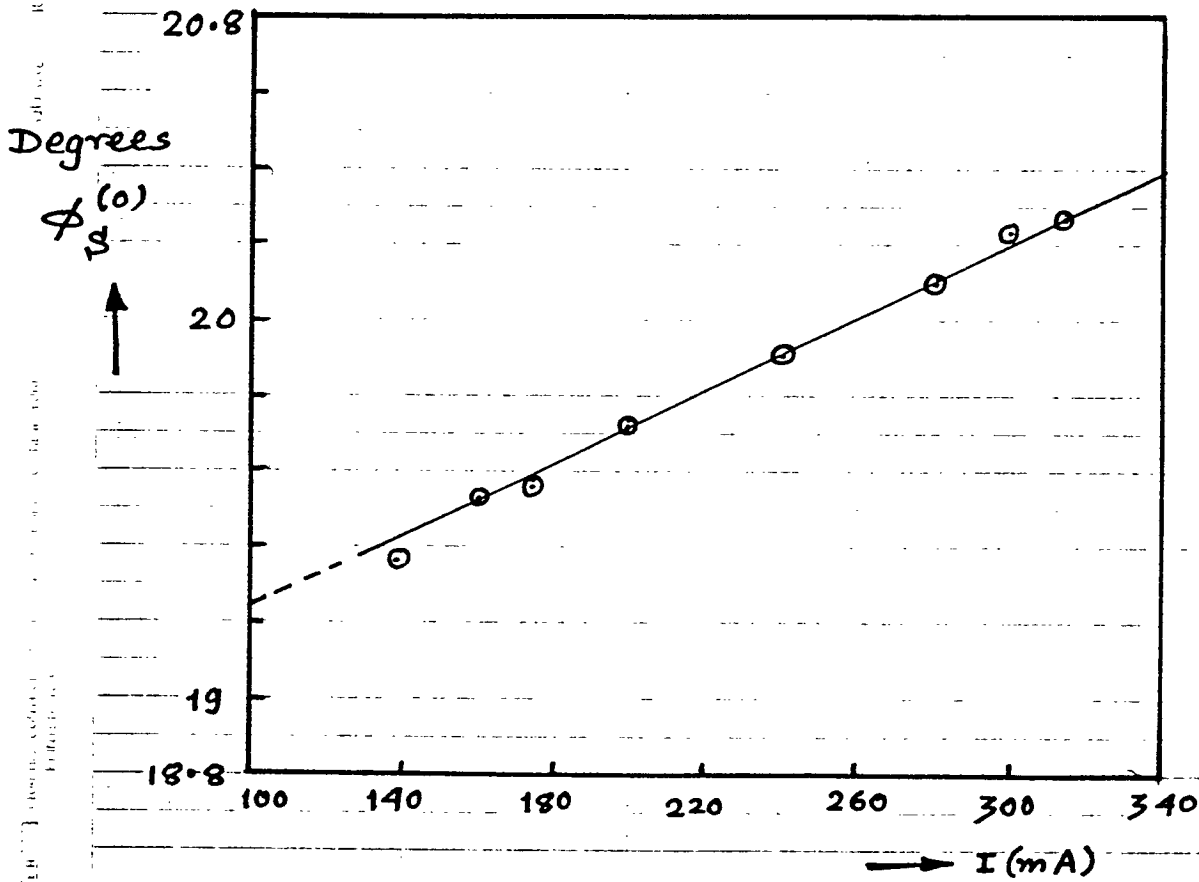
$$\frac{d\Delta\phi_s}{dI} = 2.142 \times 10^{-1} \text{ rad/Amp.}$$

Fig. 9

Single Bunch

$V_{RF} = 45.5 \text{ kV}$

$E = 744 \text{ MeV}$



$$\frac{d\Delta\phi_s}{dI} = 8.4357 \times 10^{-2} \text{ rad/Amp.}$$

Fig. 10

Resistive part of $(Z_{||}/n)$

15

The experimental value of the parasitic mode-loss factor 'k' is obtained from:

$$k = M \cdot f_0 \cdot \frac{dV_{PM}}{dI} = M \cdot f_0 \cdot V_{RF} \cos \phi_s \cdot \frac{d(\Delta \phi_s)}{dI} \quad (1)$$

where M is the number of bunches. Theoretically, for a longitudinal impedance $Z_{||}(\omega)$, the same factor is given by:

$$k = \frac{1}{2\pi} \int_{-\infty}^{+\infty} z(\omega) e^{-\omega^2 \sigma_e^2 / c^2} d\omega \quad (2)$$

for a Gaussian bunch of r.m.s. length σ_e .

Modelling the impedance by a broad-band $Q=1$ resonator with shunt impedance R_s and resonant frequency $\omega_R = 2\pi f_R$:

$$Z_{||}(\omega) = \frac{R_s}{1 - i \left(\frac{\omega_R}{\omega} - \frac{\omega}{\omega_R} \right)} \quad (3)$$

we obtain

$$k \cong \frac{R_s \omega_R}{4\sqrt{\pi}} \left(\frac{c}{\omega_R \sigma_e} \right)^3 \quad (4)$$

for $(\omega_R \sigma_e / c) \gg 1$. The $(Z_{||}/n)_{\omega=\omega_R}$ is thus obtained from k as:

$$\left(Z_{||}/n \right)_{\omega=\omega_R} = \frac{R_s}{(\omega_R/\omega_0)} = 4\sqrt{\pi} \omega_0 \omega_R \left(\frac{\sigma_e}{c} \right)^3 \cdot k \quad (5)$$

Assuming the VUV ring cut-off frequency $f_c = 1.8$ GHz to be the same as the broad-band resonator center frequency f_R , the observed slopes in Figs. 9 and 10 correspond to:

$$V_{RF} = 102.7 \text{ kV.}$$

$$R_S \cong \frac{3.25}{1.46} \text{ k}\Omega. \quad \left| \frac{Z}{n} \right|_{\omega=\omega_R}^{res.} \cong 10 \Omega.$$

$$V_{RF} = 45.5 \text{ kV.}$$

$$R_S \cong 3.7 \text{ k}\Omega. \quad \left| \frac{Z}{n} \right|_{\omega=\omega_R}^{res.} \cong 11.6 \Omega.$$

From the observed bunch lengths, one sees that the condition

$$(\omega_R \sigma_e / c) \gg 1$$

is indeed satisfied, ranging from 3.5 to 7 in all cases.

Experimentally, the scaling of parasitic mode loss with bunch length is found to be:

$$\log \left(\frac{dU_{PM}}{dI} \right)_{[eV/MA]} \cong -2.92 \log (\sigma_e)_{ns} + 8.6$$

close to the theoretically expected slope of -3, as seen from equation (1) and (4).

The above parasitic mode loss data, when converted to power vs. peak current, agrees with RF power measurements (P_{forward} - P_{reversed}, with P_{reversed} obtained from known shunt impedance of cavity locator at loss than 2.

Longitudinal Beam Transfer Function Measurement

In order to estimate the imaginary reactive component of the longitudinal beam storage ring coupling impedance, the longitudinal dipole and quadrupole (synchrotron) mode transfer functions of the beam were measured in the single bunch mode, as a function of bunch current.

The dipole mode transfer function was measured by disconnecting the two longitudinal coupled bunch feedback loop channels, but using the already existing stripline kicker and pick-up of the feedback loop to excite the bunch and observe the response. The kicker was excited with a swept frequency signal covering $52.885 \text{ MHz} \pm 12 \text{ kHz}$ thus spanning the full upper and lower first synchrotron side-bands (i.e. dipole) of the fundamental RF frequency 52.885 MHz (the synchrotron oscillation frequency is around 8.2 kHz). The signal from the longitudinal stripline vSUA pick-up and the kicker were then processed through a network analyzer to obtain the amplitude and phase response of the dipole mode. A sketch of the BTF measurement set-up for the dipole mode and the resulting expected longitudinal dipole modulation of the bunch in synchrotron phase-space and time are shown in Fig. 11 (a) and (b) respectively.

In principle the quadrupole mode could be excited by injecting the kicker with a swept frequency spanning the second synchrotron sidebands (quadrupole bands) e.g. $52.885 \text{ MHz} \pm 24 \text{ kHz}$. However the resulting induced quadrupole modulations of the beam in our set-up were barely observable above the background even with significant drive. Under this unsuccessful (and unexplainable) state of circumstances, we measured the quadrupole mode transfer function by

18

modulating the amplitude of the RF cavity instead at around twice the synchrotron frequency and observing the response at the longitudinal stripline PU. The modulation bandwidth covered a full upper quadrupole sideband. Clean quadrupole mode amplitude and phase response could be observed at the output of the network analyzer. Again the measurements were done with the longitudinal coupled bunch feedback channels disconnected. A sketch of the BTF measurement set-up for the quadrupole mode and the resulting expected longitudinal quadrupole modulation of the bunch are shown in Fig. 12 (a) and (b) respectively. Longitudinal dipole mode oscillations of the bunch can also be excited by modulating the phase of the RF cavity at around the synchrotron frequency and the resulting response observed at the longitudinal PU. This however was not done in these set of experiments.

All the response measurements were done in the single bunch mode at 744 MeV. In order to have the cleanest possible response, we used the longest available bunch lengths by choosing the lowest RF voltage, namely $V_{RF} = 45.5$ kV. In order to interpret the response data in terms of linear perturbative response formalism, we used the minimum amount of drive (i.e. excitation) needed to just clearly observe the response and no more.

A typical quadrupole mode amplitude and phase response observed on the network screen is shown in Fig. 13. Observed dipole mode response at five different average currents up to $I = 31$ mA are shown in Fig. 14 (a)-(e). Observed quadrupole response at seven different average currents up to $I = 22.5$ mA are shown in Fig. 15 (a)-(g).

Fig. 11 (a) Dipole mode BTF measurement set up and (b) expected bunch modulations.

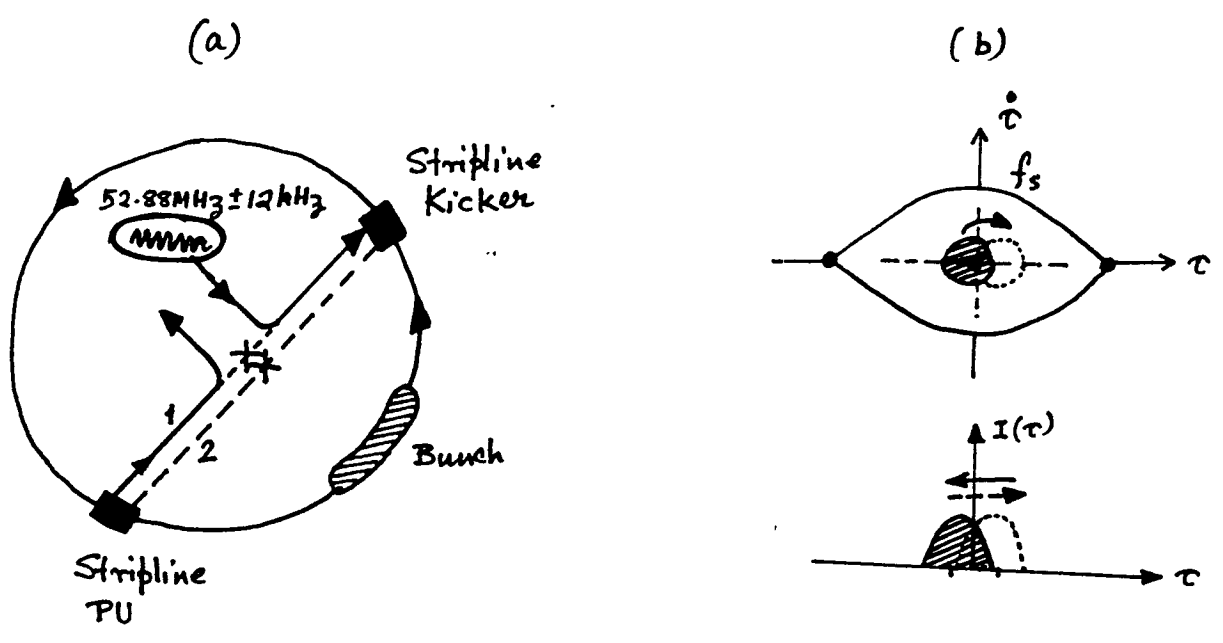
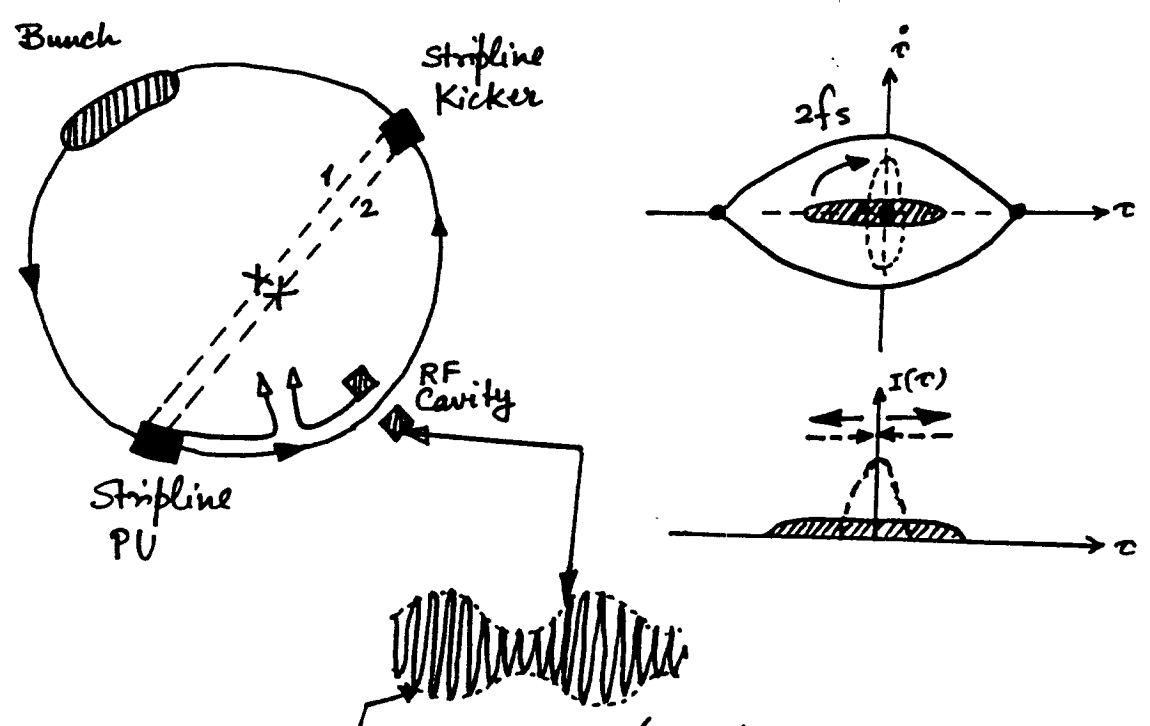
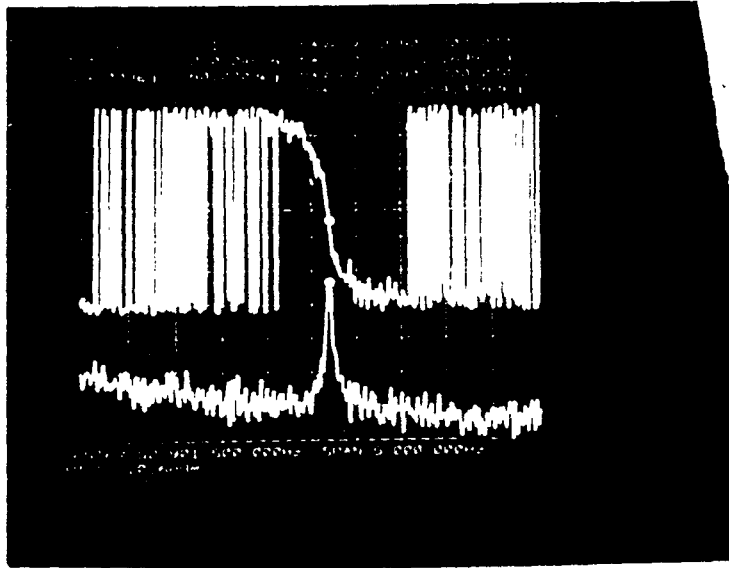


Fig. 12 (a) Quadrupole mode BTF measurement set up and (b) expected bunch modulations.



$E = 744 \text{ MeV}$
 $I = 4 \text{ mA}$
 $V_{RF} = 45.5 \text{ kV}$



A typical quadrupole mode amplitude (bottom curve) and phase (top curve) response observed on the network analyzer screen.

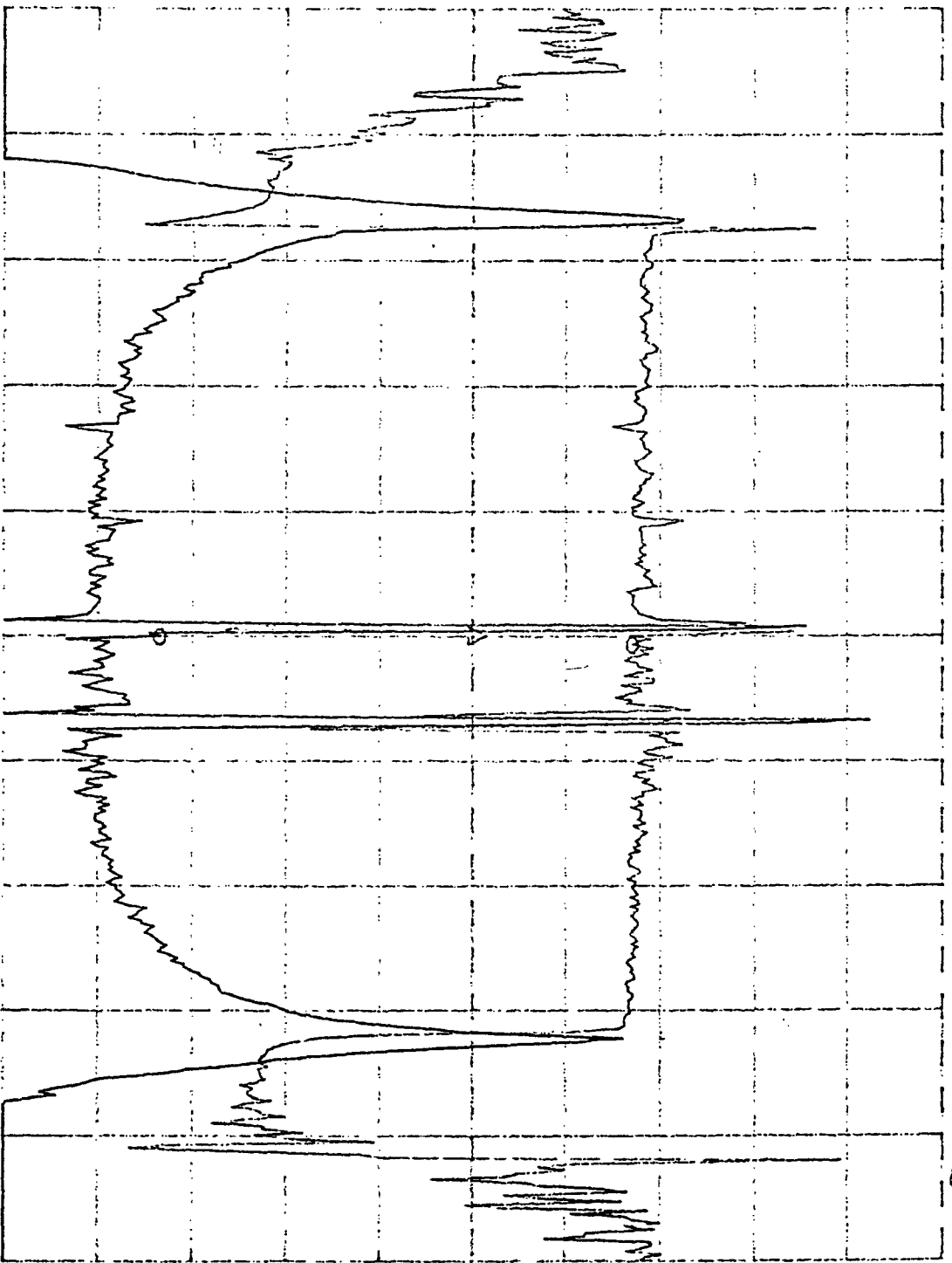
Fig. 13

W/ptc 2E1

I = 0.2 mA
RF = 200

11/19/85
23:40

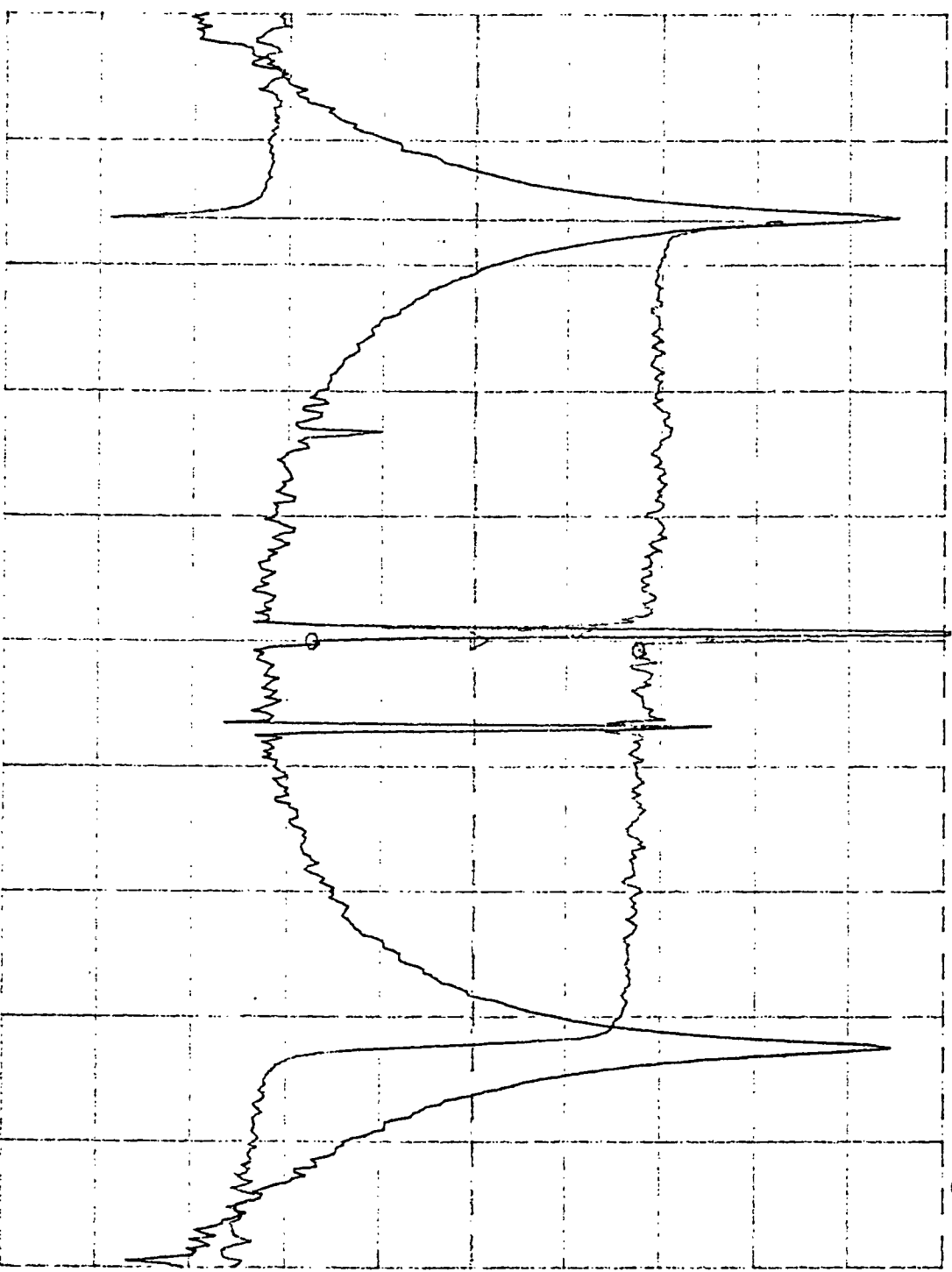
REF LEVEL /DIV MARKER 52 885 784.038Hz
 -40.000dB 5.000dB MAG (S21) -81.762dB
 -239.500deg 45.000deg OFFSET 187.500Hz
 PHASE (S21) 75.675deg



CENTER 52 885 784.038Hz SPAN 25 000.000Hz
 AMP TD 15.0dBm

Fig. 14(a)

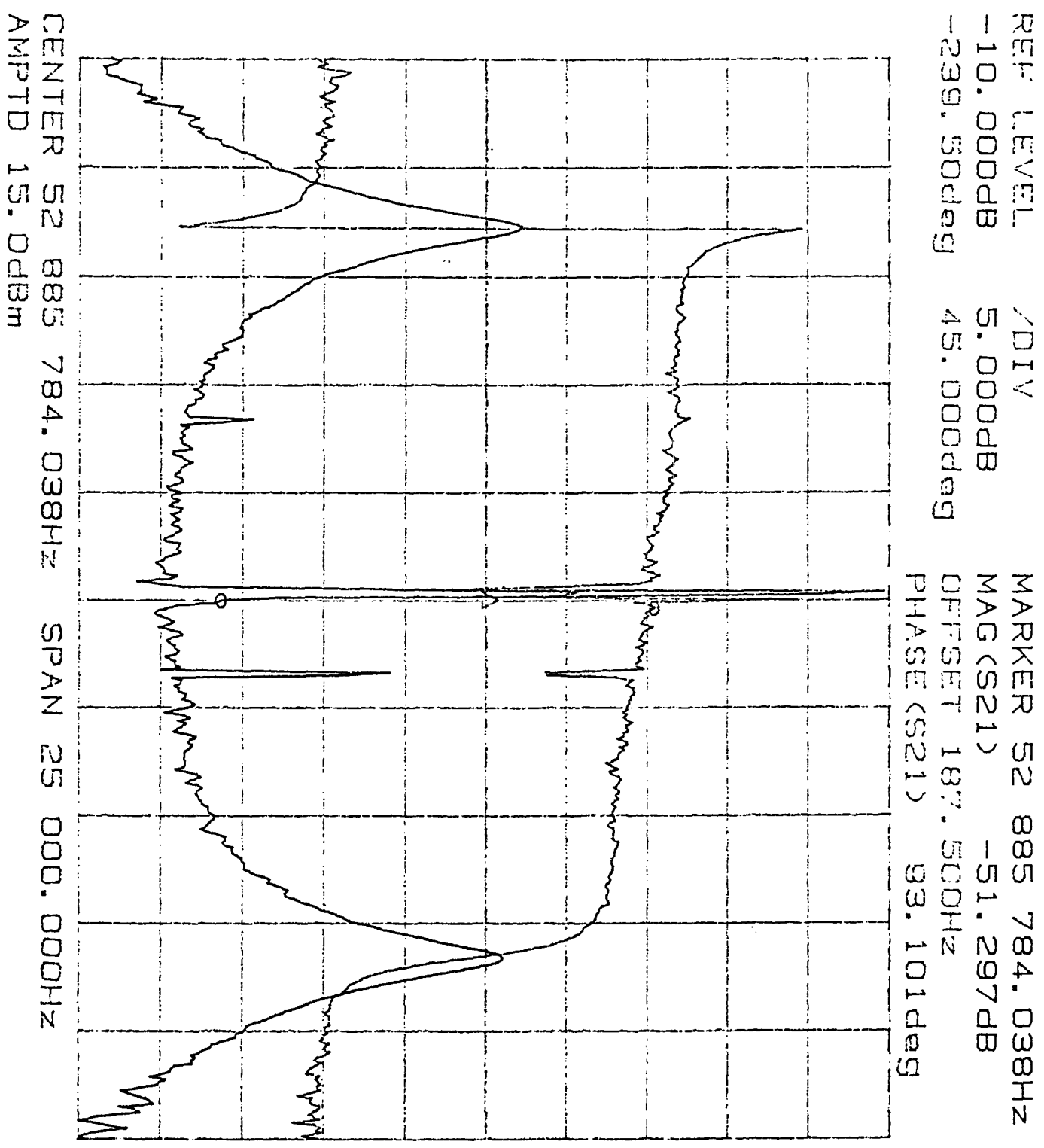
REF LEVEL /DIV MARKER 52 885 784.038Hz RF = 200
 -30.000dB 5.000dB MAG(S21) -63.727dB
 -239.50deg 45.000deg OFFSET 187.500Hz
 PHASE(S21) 78.216deg



I = 5 mA

11/19/85
23:55

Fig. 14(b)

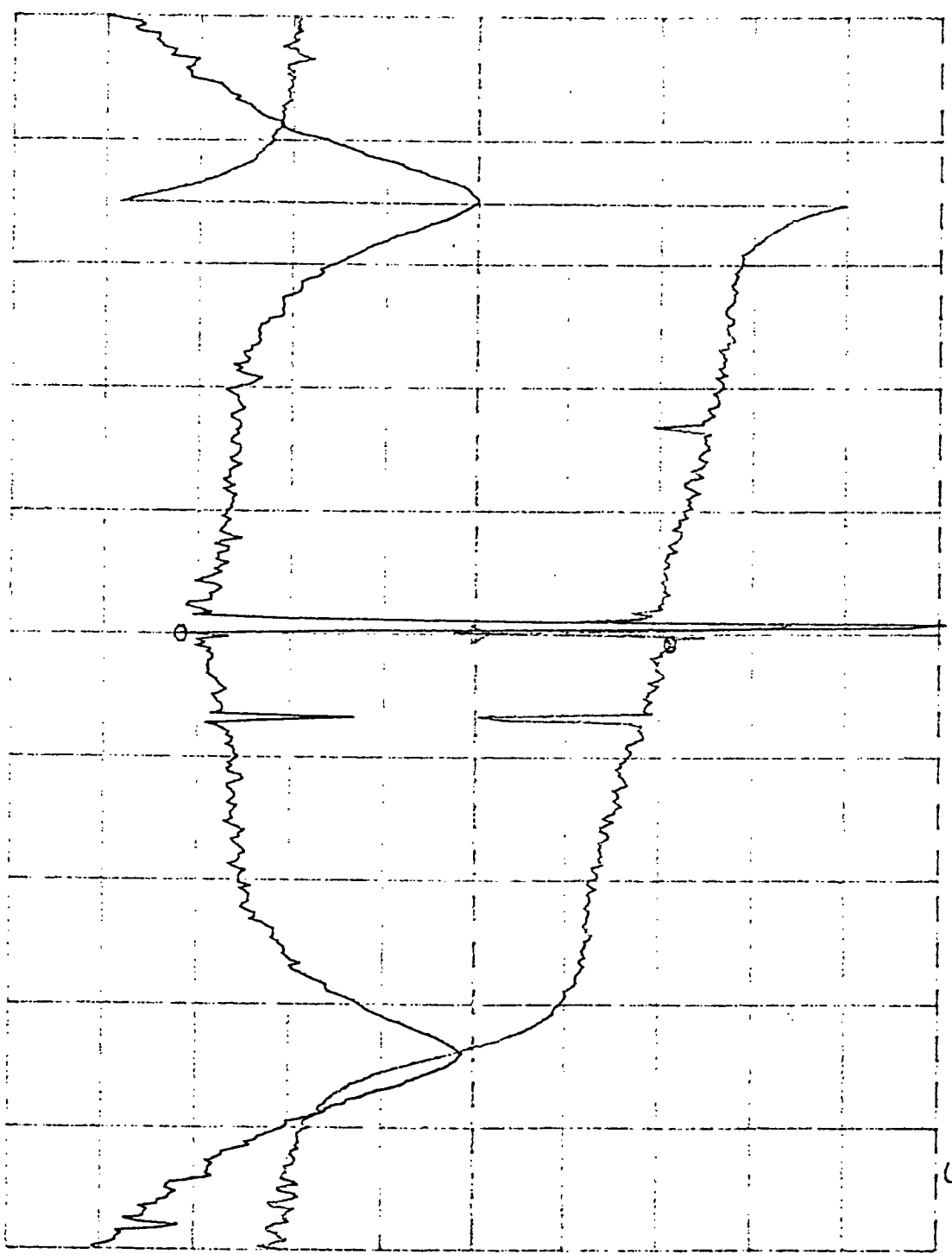


I=12m#

RF=200

Fig. 14(c)

REF LEVEL /DIV MARKER 52 885 784.038HZ
 -10.000DB 5.000DB MAG(S21) -50.891DB
 -239.50deg 45.000deg OFFSET 187.500HZ
 PHASE(S21) 94.191deg

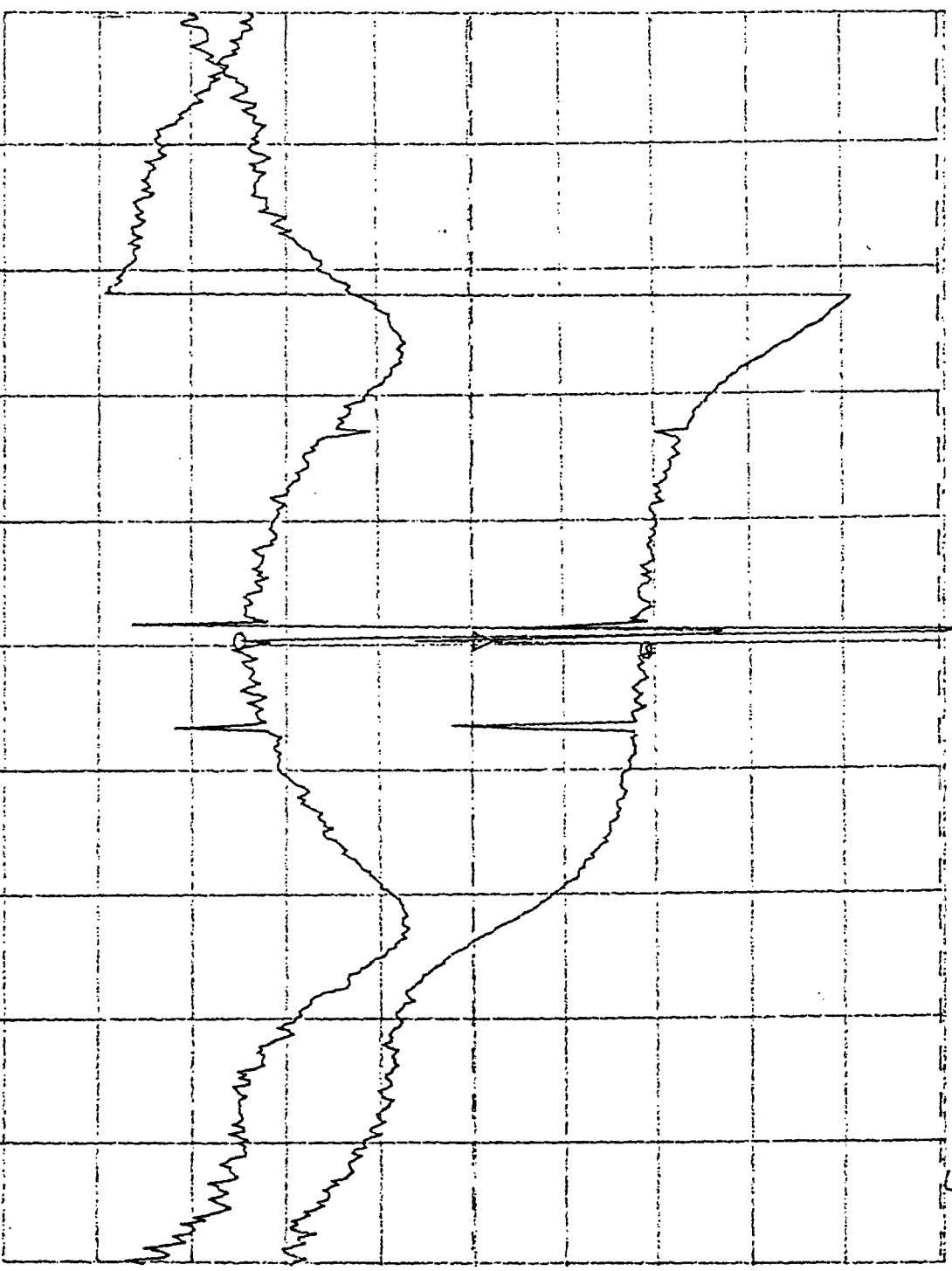


CENTER 52 885 784.038HZ SPAN 25 000.000HZ
 AMP TD 15.0dBm

I = 21 mA
 R_F = 200
 23:40
 11/11/82

Fig. 14(a)

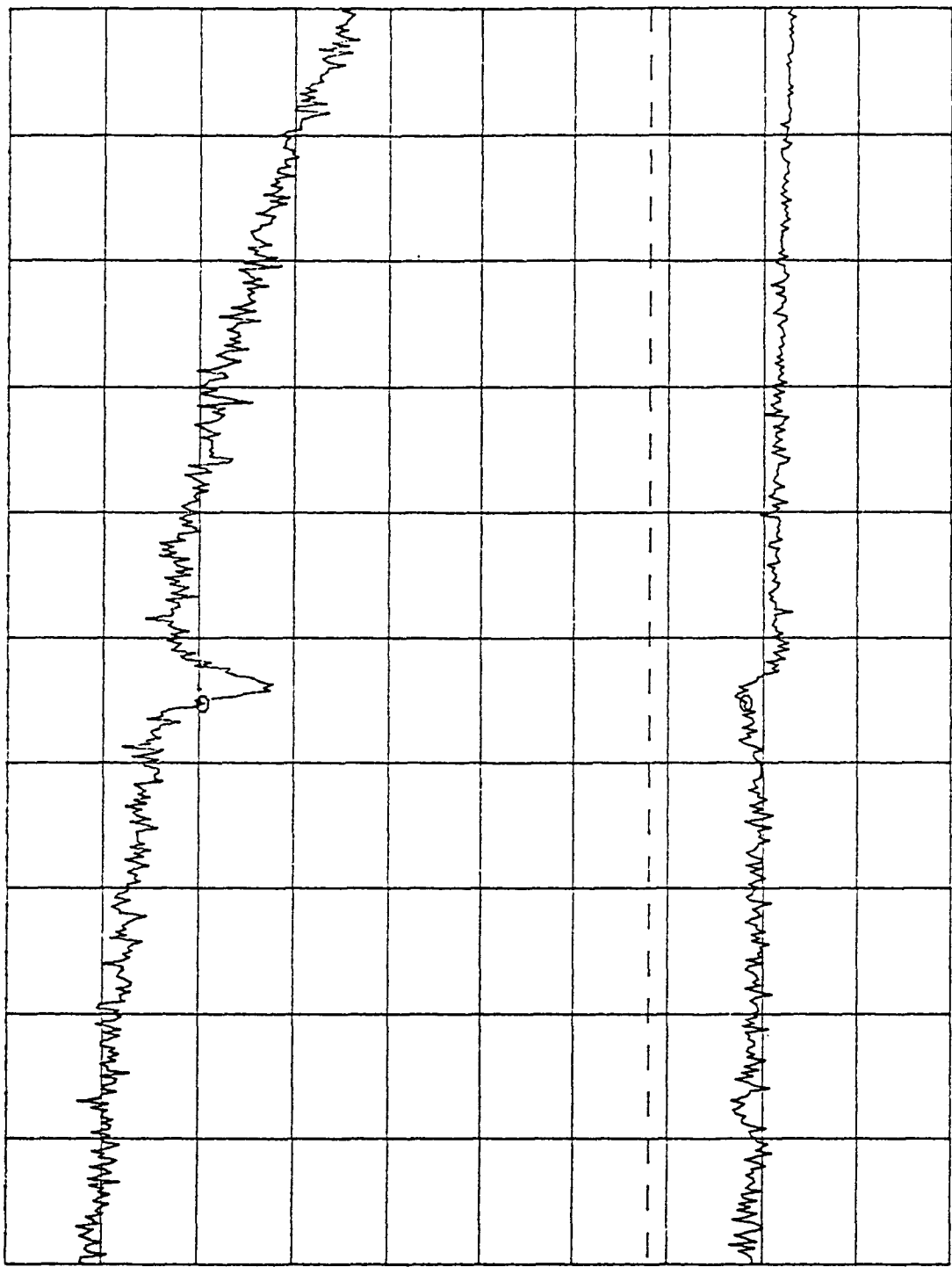
REF LEVEL /DIV MARKER 52 885 784.038Hz
 -10.000dB 5.000dB MAG (S21) -47.673dB
 -239.500deg 45.000deg OFFSET 187.500Hz
 PHASE (S21) 81.564deg



CENTER 52 885 784.038Hz SPAN 25 000.000Hz
 AMP TD 15.00dBm

Fig. 14(c)

REF LEVEL /DIV MARKER 52 901 762.500HZ
 0.0 200.00E-6 MAG (S21) 408.32E-6
 329.00deg 60.000deg MARKER 52 901 762.500HZ
 PHASE (S21) 29.918deg



CENTER 52 901 500.000HZ SPAN 5 000.000HZ
 AMP TD 10.6dBm

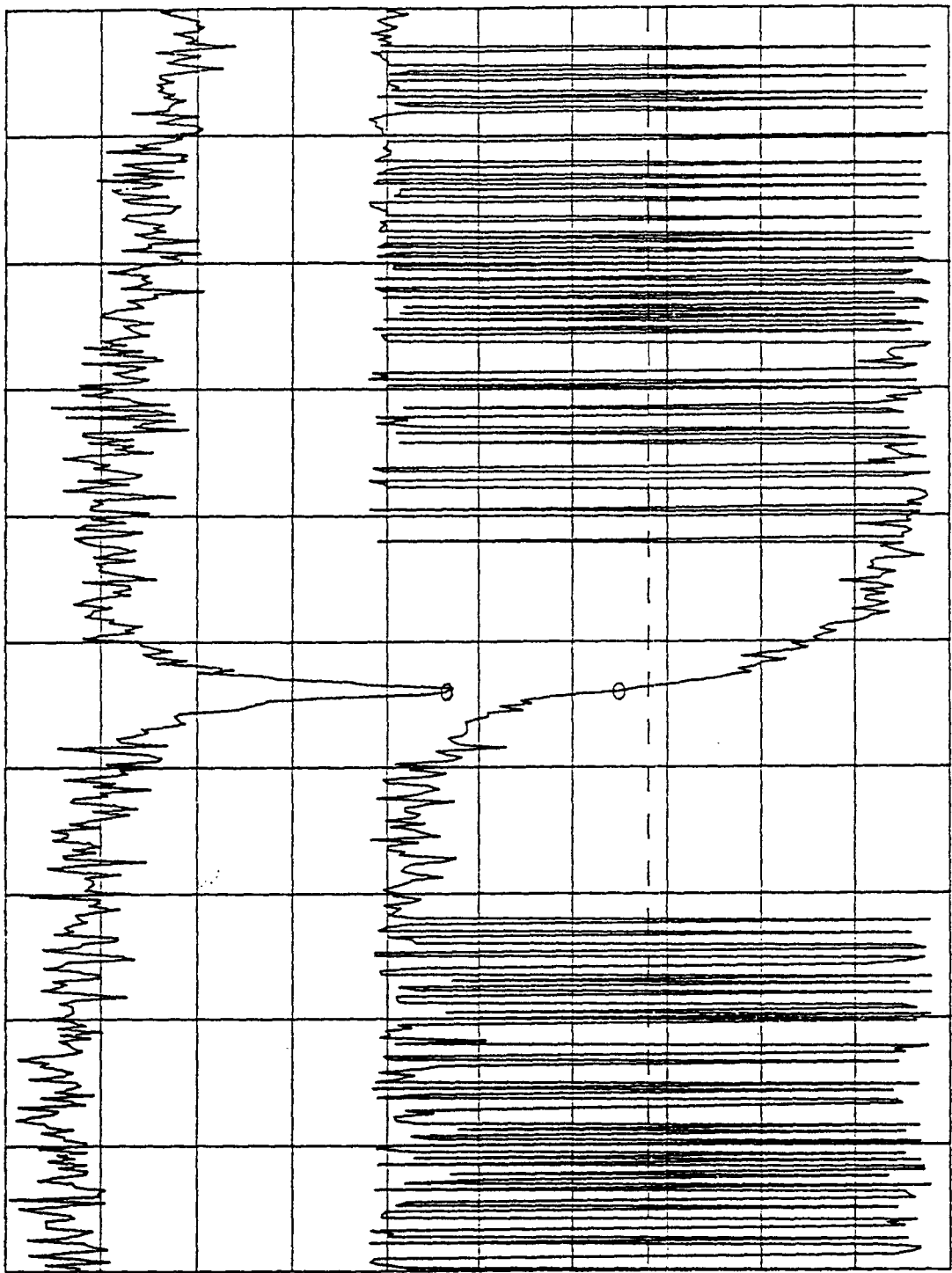
J = 1mA

44dB

(PF 200)

Fig. 15 (a)

REF LEVEL /DIV MARKER 52 901 700.000HZ
 0.0 250.24E-6 MAG (S21) 1.1639E-3
 224.00deg 60.000deg MARKER 52 901 700.000HZ
 PHASE (S21) -154.476deg

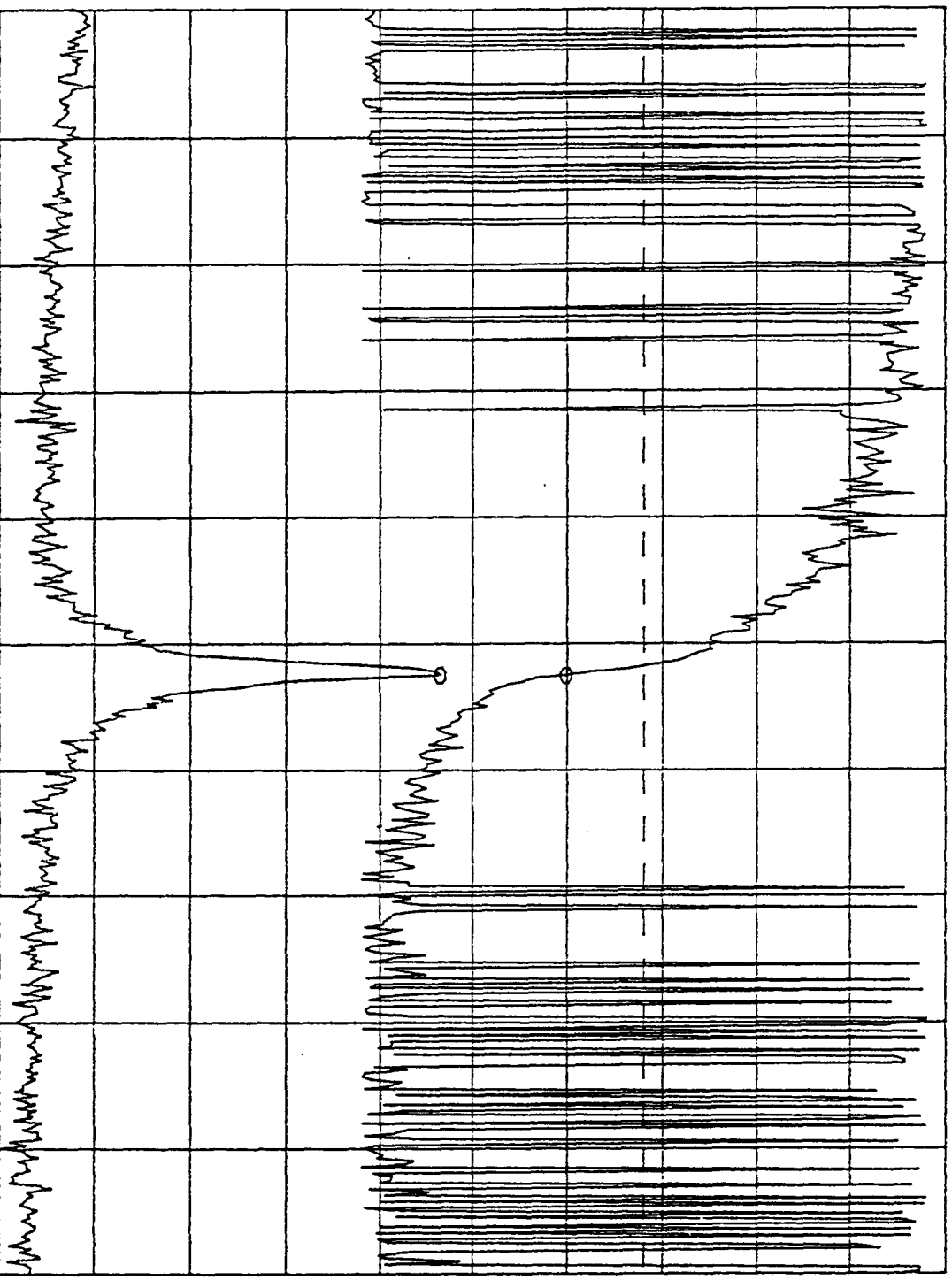


CENTER 52 901 500.000HZ SPAN 5 000.000HZ
 AMP TD 10.6dBm

Fig. 15 (b)

7:41

REF LEVEL /DIV MARKER 52 901 625.000HZ
 0.0 1.0000E-3 MAG (S21) 4.6496E-3
 224.00deg 60.000deg MARKER 52 901 625.000HZ
 PHASE (S21) 175.407deg

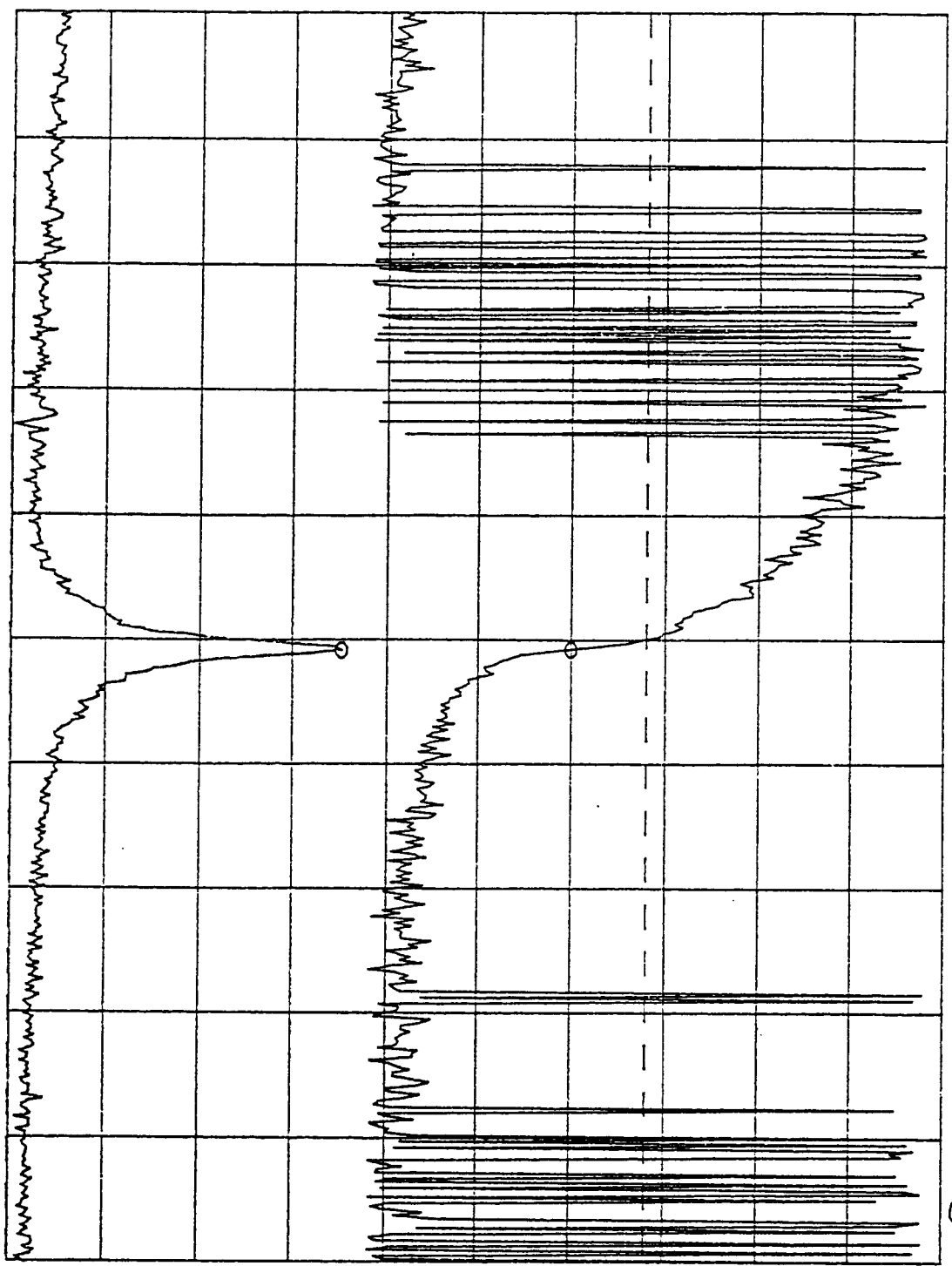


CENTER 52 901 500.000HZ SPAN 5 000.000HZ
 AMP TD 10.6dBm

$I = 9mA$
 5.6dB
 P.F. 21.7

Fig. 15 (c)

REF LEVEL /DIV 2.4570E-3
 0.0 60.000deg
 221.00deg
 MARKER 52 901 537.500HZ
 MAG (S21) 8.6436E-3
 MARKER 52 901 537.500HZ
 PHASE (S21) 172.786deg



CENTER 52 901 500.000HZ
 AMP TD 10.6dBm
 SPAN 5 000.000HZ

Fig. 15 (d)

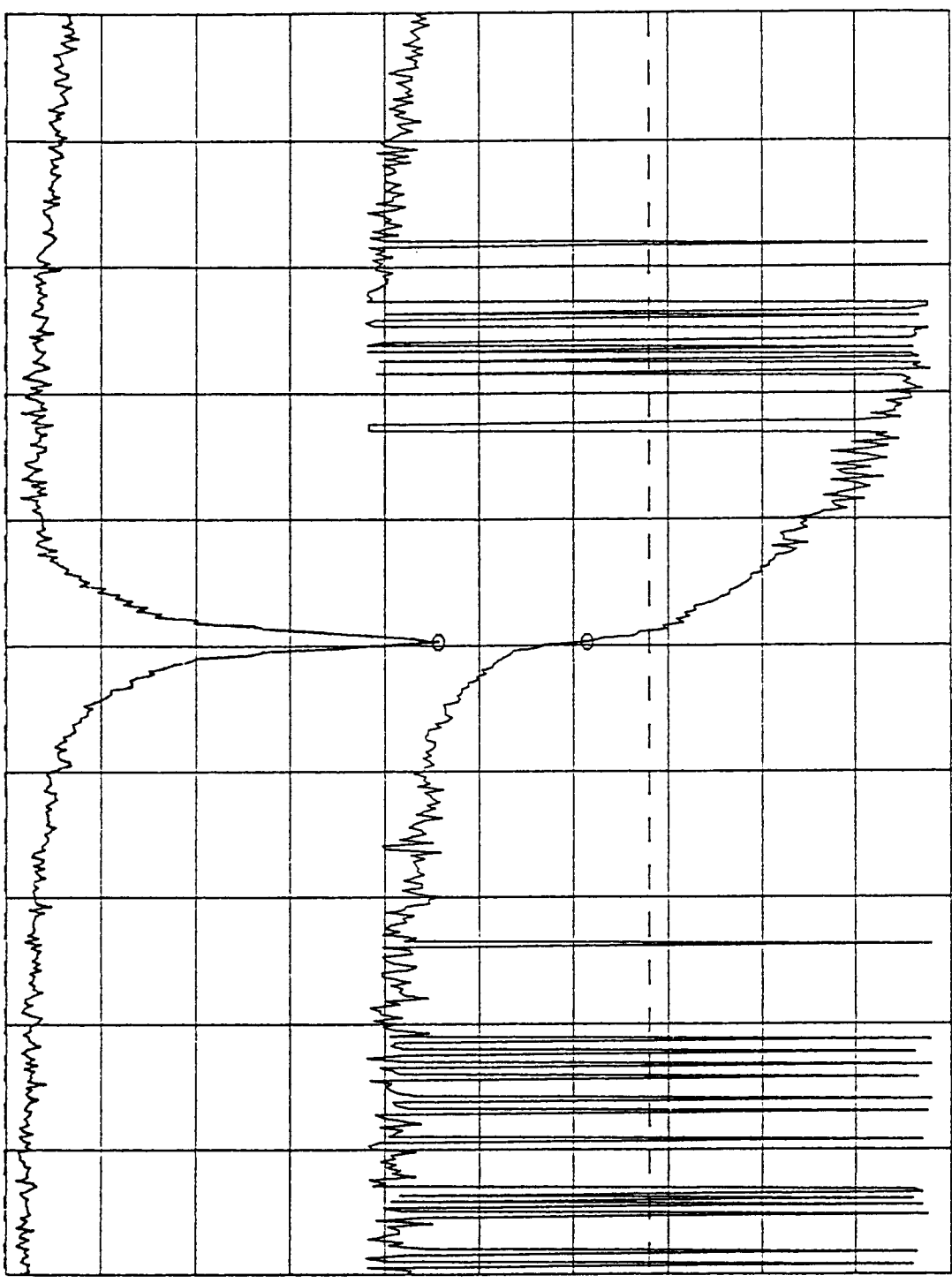
J = 15 m H
 56 f H,
 RF 2000

2

REF LEVEL 0.0
224.00deg

/DIV 2.5355E-3
60.000deg

MARKER 52 901 487.500HZ
MAG(S21) 11.601E-3
MARKER 52 901 487.500HZ
PHASE(S21) -175.369deg



CENTER 52 901 500.000000 HZ
SPAN 5 000.000000 HZ
AMP TD 10.6dBm

52 20 mA

58dBm
RF 2.000

Fig. 15 (e)

REF LEVEL 0.0
 /DIV 10.000E-3
 224.00deg 60.000deg
 MARKER 52 901 500.000HZ
 MAG (S21) 25.660E-3
 MARKER 52 901 500.000HZ
 PHASE (S21) -173.447deg

CENTER 52 901 500.000HZ SPAN 5 000.000HZ
 AMP TD 10.6dBm

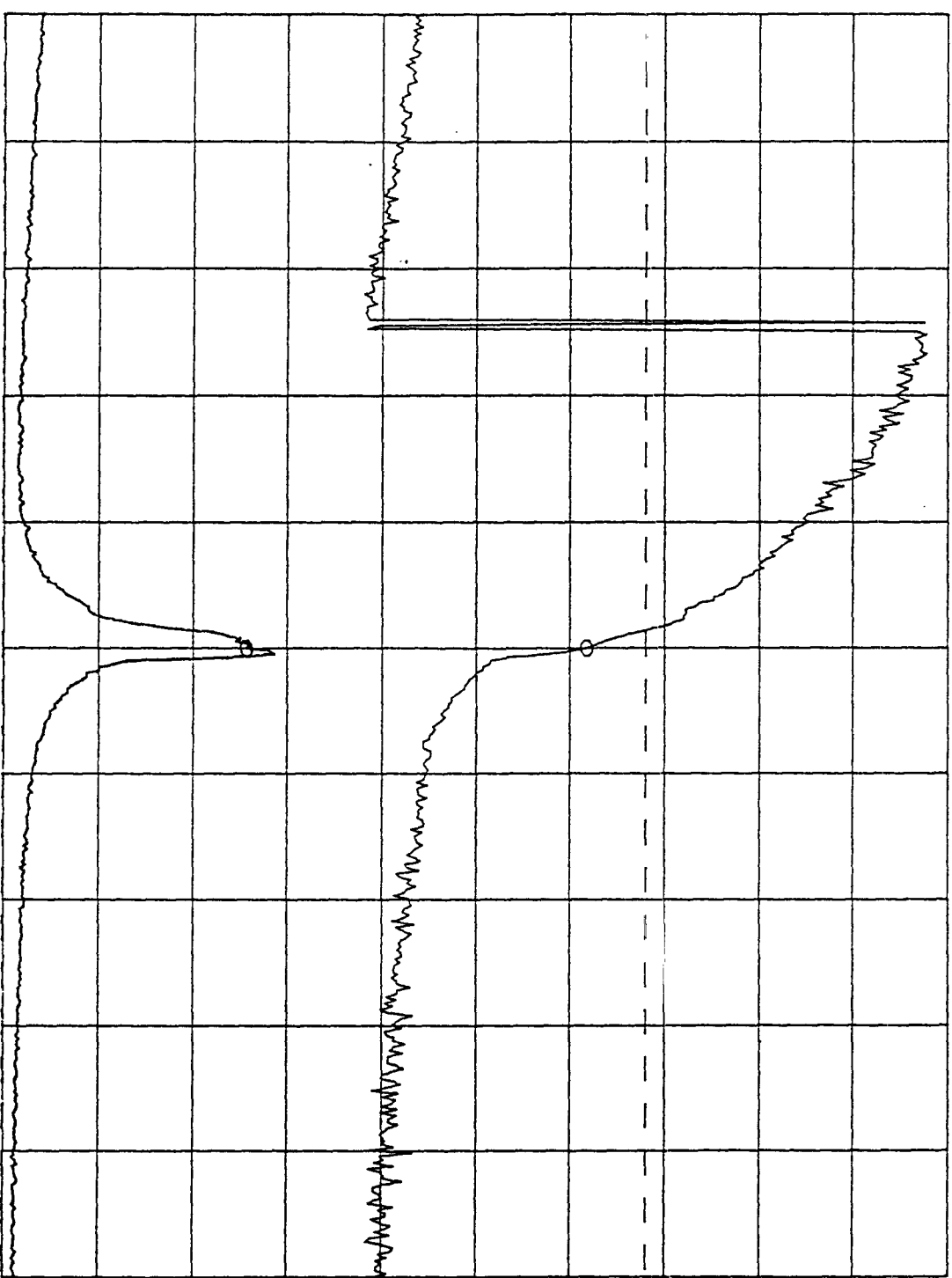
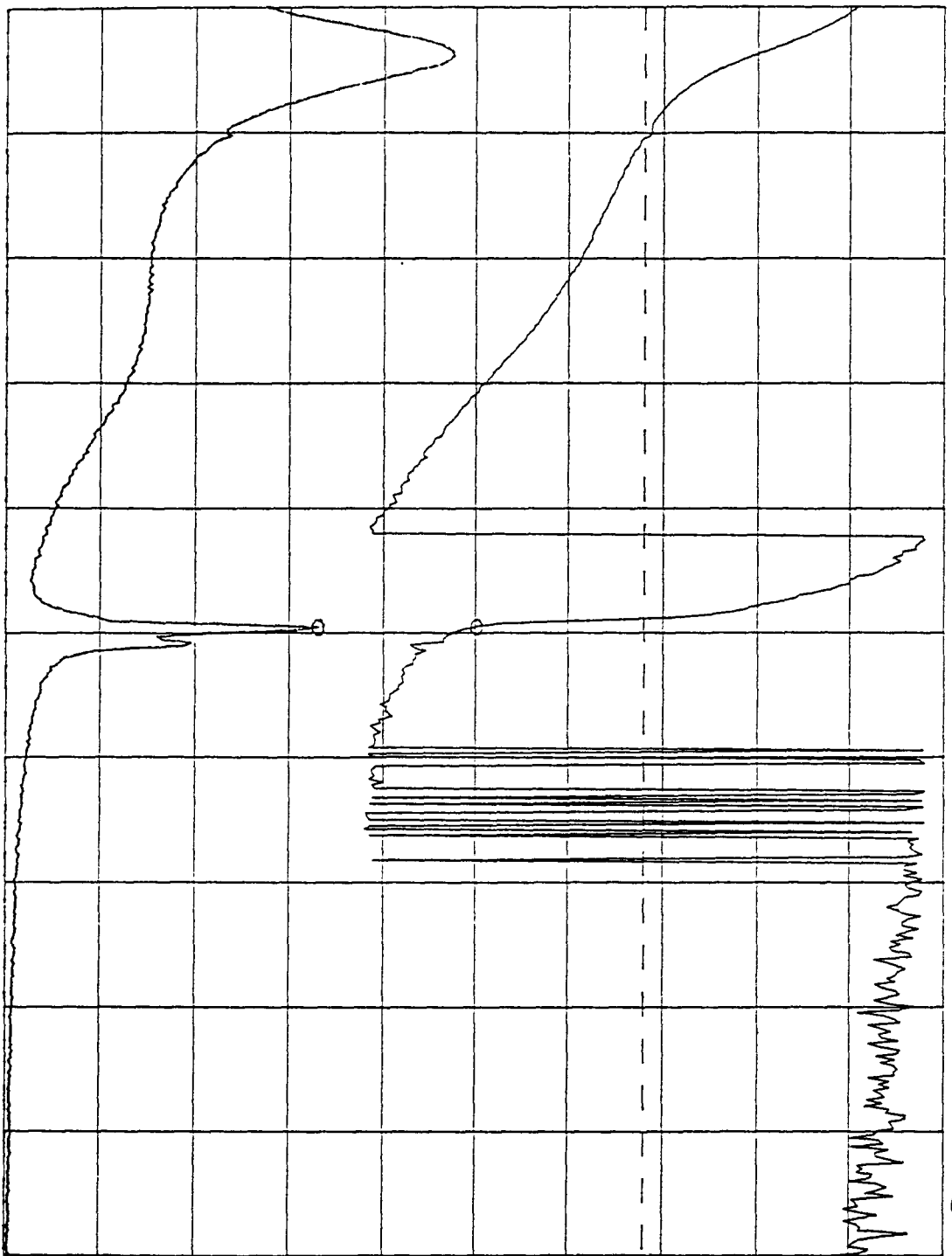


Fig.15(e)

REF 200
 setting of 50dB
 att

REF LEVEL 0.0
 235.00deg
 /DIV 20.000E-3
 60.000deg
 MARKER 52 901 400.000HZ
 MAG (S21) 66.206E-3
 MARKER 52 901 400.000HZ
 PHASE (S21) 127.896deg



CENTER 52 901 500.000HZ
 AMP TD 10.6dBm
 SPAN 20 000.000HZ

I ≈ 22.4 mA
 P ≈ 250

Fig. 15 (f)

In all cases the phase response has the physically expected features of constant phase far outside the band of incoherent frequencies (synchrotron) occupied by the beam and a phase jump (e.g. by 180° for the dipole) across the band. The maximum of the amplitude response curve corresponds to the coherent dipole or quadrupole mode frequency of the bunch, while the frequency width over which the phase jump occurs is a measure of the incoherent synchrotron frequency spread in the bunch.

The coherent dipole and quadrupole mode frequencies of the single bunch as a function of beam current are plotted in Fig. 16. The measured slopes of the coherent frequency vs. current correspond to:

$$\text{Dipole Mode: } (f_c)_d = 8.175 + 21.17 \times I \text{ [amp]} \quad [\text{kHz}]$$

$$2 \cdot (f_c)_d = 16.35 + 42.34 \times I \text{ [amp]} \quad [\text{kHz}]$$

$$d(f_c)_d/dI = +21.17 \text{ kHz/Amp}$$

$$\text{Quadrupole Mode: } (f_c)_q = 16.51 - 15.55 \times I \text{ [amp]} \quad [\text{kHz}]$$

$$d(f_c)_q/dI = -15.55 \text{ kHz/Amp.}$$

Single Bunch.
 $V_{RF} = 45.5 \text{ kV}$
 $E = 744 \text{ MeV}$

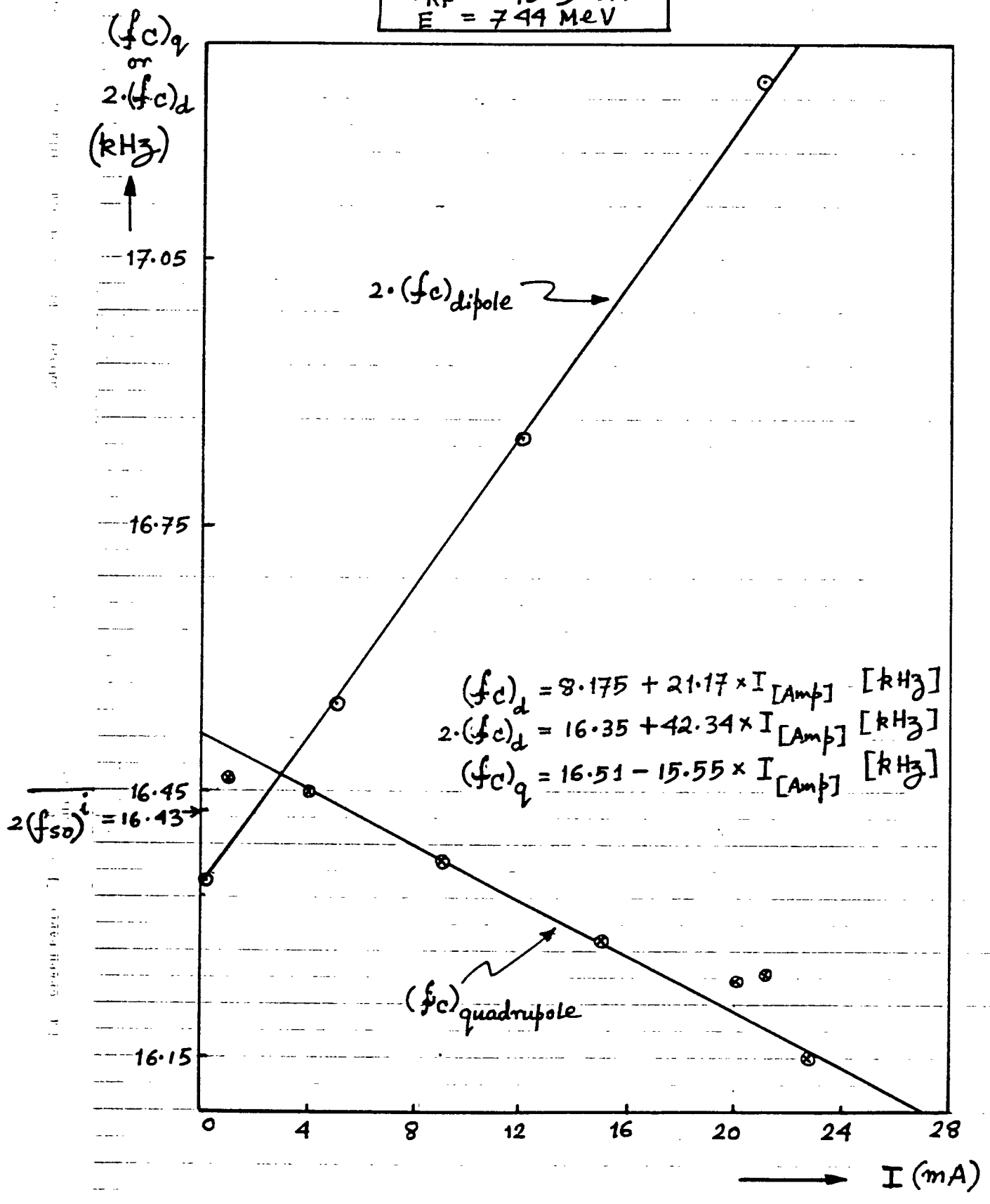


Fig. 16

Reactive part of $(Z_{||}/n)$

35

The imaginary reactive part of $Z_{||}(\omega)$ will change the incoherent and coherent oscillation frequencies. The slope of the coherent frequency vs. current contains information about $\text{Im}(Z_{||}/n)$.

In order to extract $\text{Im}(Z_{||}/n)$, we have to interpret the coherent freq. vs. current data very carefully. The bunch will induce longitudinal voltage through the reactive component of $(Z_{||}/n)$, and thus distort the focusing longitudinal potential well that confines the bunch. The reactive part will thus lead to a shift of the incoherent synchrotron frequency with increasing current. This potential well distortion which affects the zero order stationary beam dynamics is expected to influence the coherent dipole motion very weakly, since the distortion is confined within and moves with the bunch. The effect on the quadrupole mode is expected to be stronger since there is no macroscopic motion of the bunch centroid in the quadrupole mode.

If this were the only effect, we would observe a flat dipole mode coherent frequency as a function of beam current with zero slope and a finite slope for the quadrupole mode coherent frequency vs. current, whose sign would depend on whether the bunch samples mostly the inductive or capacitive part of the impedance. However this effect is slightly perturbed by the linear perturbative coherent

36.

frequency shift of the already distorted (potential-well wise) stationary bunch. This will lead to a nonzero shift of the coherent dipole frequency and the same effect will also affect the quadrupole mode coherent frequency away from the potential-well distorted coherent effect. We have to subtract this latter effect away in order to extract $\text{Im}(Z_{11}/n)$ from the pure potential-well induced quadrupole mode shift.

In Fig. 17 we superimpose the model broadband impedance of the ring centered at the cut-off frequency $f_c = 1.8 \text{ GHz}$, ~~the~~ below the frequency spectrum of the DC, dipole and quadrupole mode of the bunch. The envelopes of the mode spectrum peak when $(\omega\tau_{1/2})$, the argument of the Bessel function is of the same magnitude as the order of the Bessel function. Thus dipole mode peaks at $\omega\tau_{1/2} \sim 1$ and quadrupole mode at $\omega\tau_{1/2} \sim 2$, etc., where $\tau_{1/2}$ is the full half-length of the bunch. For currents upto 30 mA, we may take the bunch length to be the natural bunch length at zero intensity. From the known bunch length data, we then find that the dipole peaks at a frequency of 0.53 GHz and the quadrupole mode peaks at a frequency of about 1 GHz, far below the cut-off of 1.8 GHz. The bunch thus sample mostly the low frequency inductive region

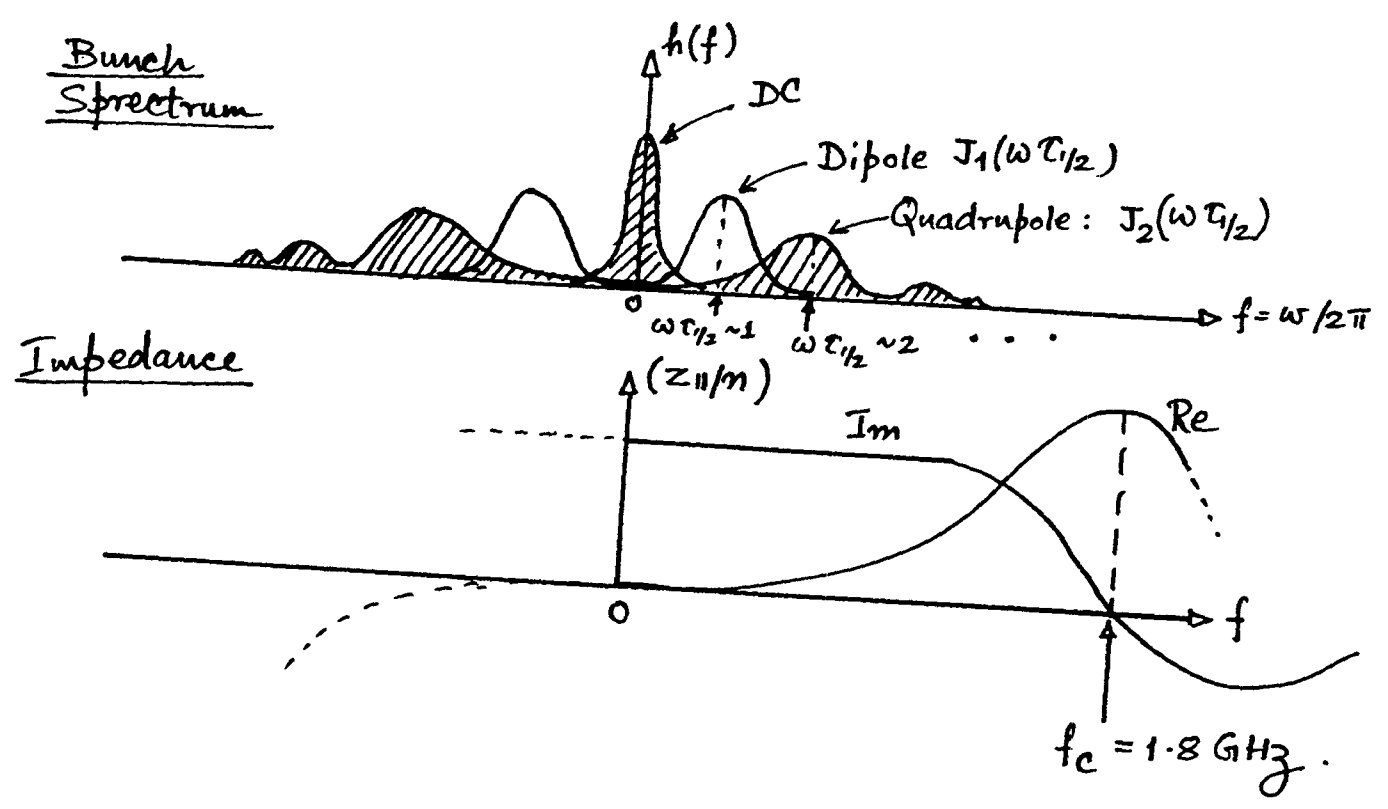


Fig. 17.

of the impedance, where $(Z_{||/m})$ is approximately constant.

From the known expression for the linear perturbative coherent frequency shift, given by⁽³⁾

$$\begin{aligned}
 (\Delta\omega_{||})_m &= -i \frac{m\omega_s}{(m+1)} \frac{I_0}{3Vh \cos\phi_s} \left(\frac{J_1}{\omega_0\tau_{1/2}}\right)^3 \frac{\sum_n \frac{Z_{||}(n\omega_s + m\omega_s)}{n} h_{mm}^{(n)}(m\omega_s)}{\sum_n h_{mm}(n\omega_s)} \\
 &= -i \frac{m\omega_s}{(m+1)} \frac{I_0}{3Vh \cos\phi_s} \left(\frac{J_1}{\omega_0\tau_{1/2}}\right)^3 \left(\frac{Z_{||}}{n}\right)_0^{\text{reac.}}
 \end{aligned}$$

we can assume then that ratio of the linear coherent perturbative shift for quadrupole and dipole modes, is

$$\frac{(\Delta\omega_{||})_{m=2}}{(\Delta\omega_{||})_{m=1}} = \frac{2/3}{1/2} = \frac{4}{3},$$

for the same $Q(Z_{||}/n)$. We then subtract the full dipole mode slope from the dipole curve and (4/3) the dipole mode slope from the quadrupole curve in Fig. 16. The resulting curves are shown in Fig. 18, which now contains information of the pure potential-well distortion effect of the quadrupolar mode.

The change of incoherent synchrotron frequency due to potential-well distortion by inductive impedance is given by: (4)

$$f_s^i = f_{s0}^i \left[1 - \frac{3I_0}{M \cdot 2\pi^2 h V_0 \cos\phi_s} \left(\frac{2\pi R}{l} \right)^3 \left(\frac{Z}{n} \right)_0^{\text{react.}} \right]$$

where M is the number of bunches and l the total bunch length. The corresponding slope is:

$$\frac{df_s^i}{dI} = - \frac{3f_{s0}^i}{M \cdot 2\pi^2 h V_0 \cos\phi_s} \left(\frac{2\pi R}{l} \right)^3 \left(\frac{Z}{n} \right)_0^{\text{react.}}$$

Incoherent frequencies are hard to measure from the response curves. Rather the coherent frequency is measured more accurately. In the limit of zero synchrotron frequency spread, the effect on the coherent quadrupole mode is given by: (5)

$$\delta(f_c)_q \xrightarrow{\Delta f_s \rightarrow 0} \frac{1}{4} \delta f_s^i$$

Then

$$\frac{d(f_c)_q}{dI} = \frac{1}{4} \frac{df_s^i}{dI} = - \frac{3f_{s0}^i}{M \cdot 2\pi^2 h V_0 \cos\phi_s} \left(\frac{2\pi R}{l} \right)^3 \left(\frac{Z}{n} \right)_0^{\text{react.}}$$

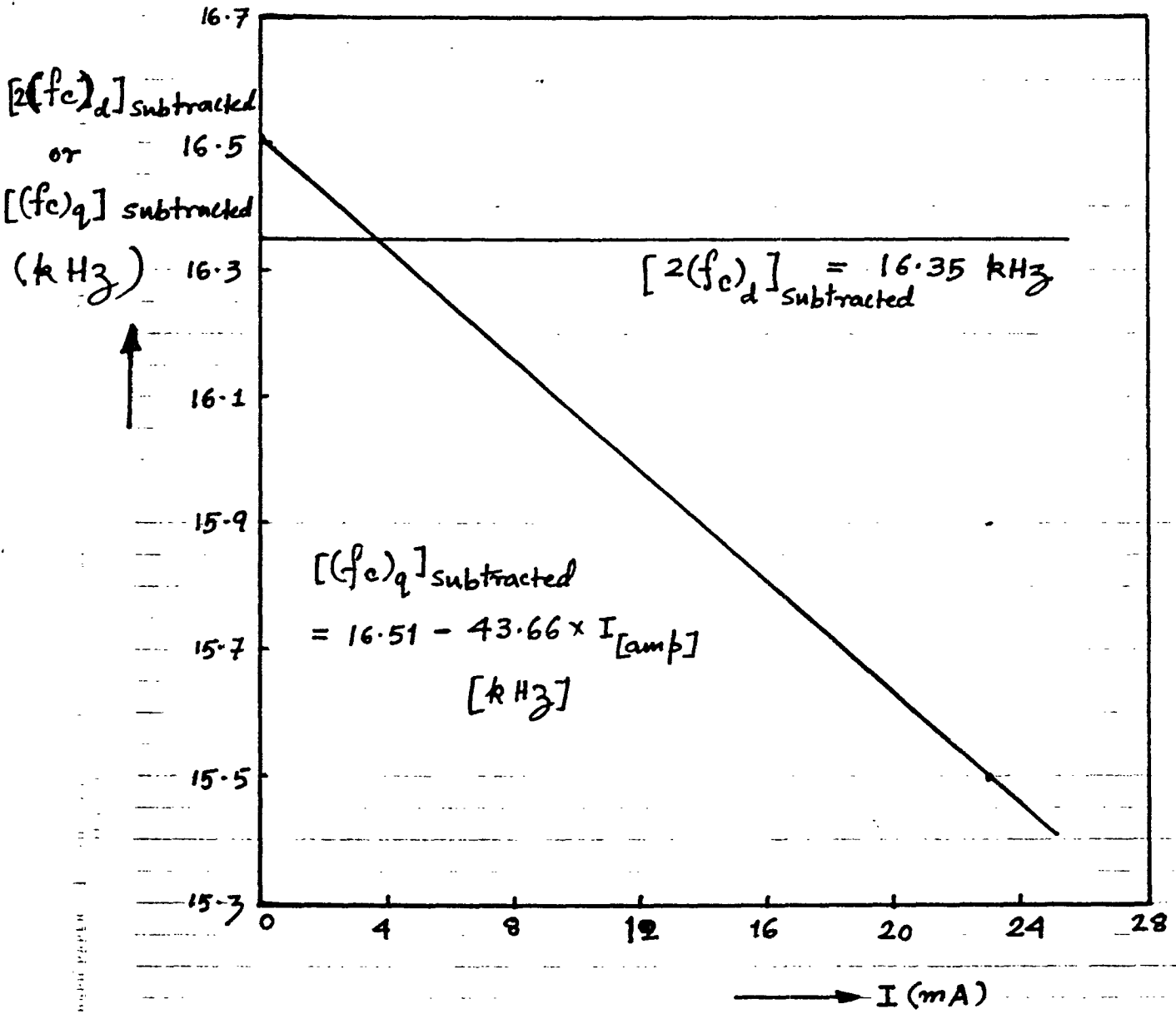


Fig. 18

Synchrotron Freq. Spread
vs.
Beam Current.

[Derived from quadrupole mode phase-jump]

$$(\Delta f_s) = \frac{(\Delta f) \Delta \phi = 2\pi}{2}$$

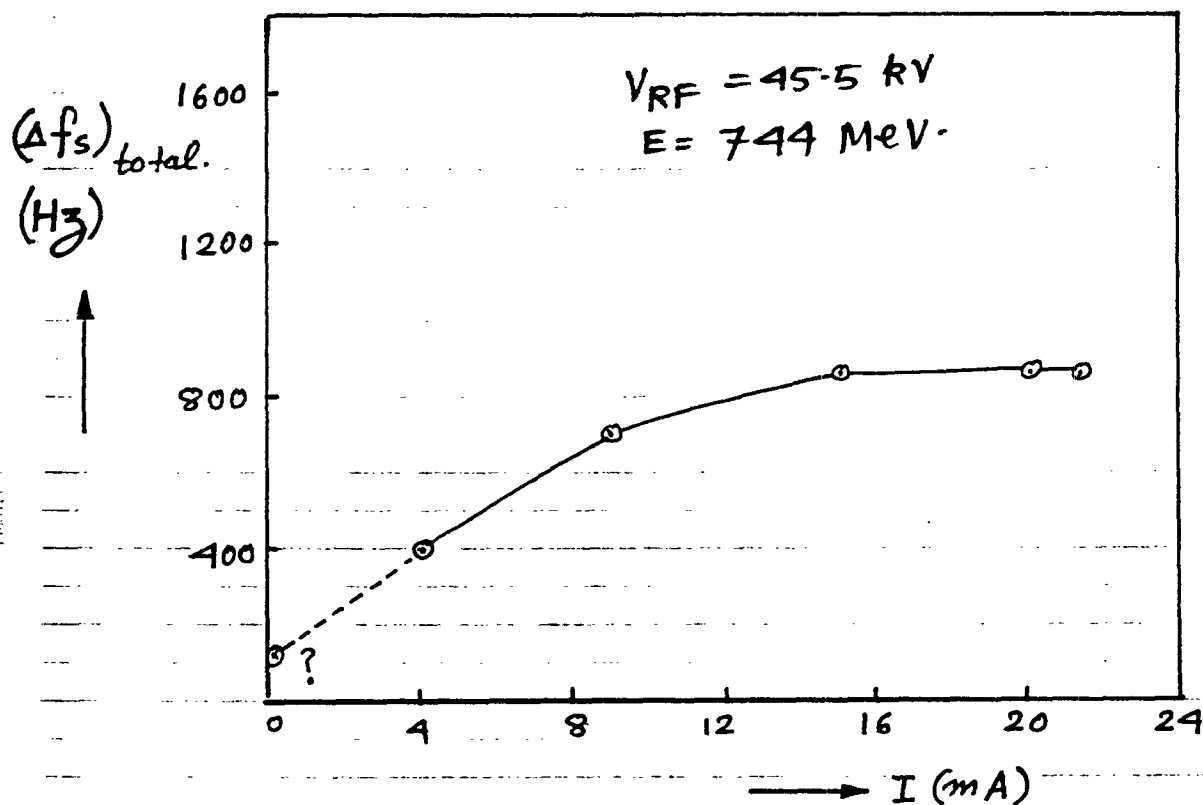


Fig. 19

Bunch Length Derived from Synchrotron Freq. Spread.

For bunches occupying a small fraction of the bucket, we can assume the following octupolar dependence of synchrotron frequency on the synchrotron oscillation amplitude 'a' in actual angle around the storage ring:

$$f_s^i = f_{s0}^i \left(1 - \frac{h a^2}{16}\right)$$

where h is the RF harmonic Number. This is true provided the RF waveform is not distorted away from the sinusoidal shape. The full bunch length in time is then:

$$\begin{aligned} (\Delta\tau)_{total} &= \frac{R}{c} \cdot (\Delta\theta)_{max} = \frac{R}{c} (2a_{max}) \\ &= \frac{8}{h} \left(\frac{\Delta f_s}{f_{s0}}\right)^{1/2} \frac{R}{c} \end{aligned}$$

A sample calculation for $V_{RF} = 45.5 \text{ kV}$ at $I = 4 \text{ mA}$ where $\Delta f_s = 400 \text{ Hz}$ and $f_{s0} = 8.375 \text{ kHz}$

yields

$$(\Delta\tau)_{tot.} \approx 5 \text{ ns.}$$

The rms. bunch length observed is $\sigma_L = .21 \text{ ns}$ giving a $(\Delta\tau)_{tot}$ of $.714 \text{ ns}$.

The discrepancy by a factor of seven is partly due to the fact that the phase response is extremely sensitive even to the tails of a Gaussian bunch and

probably overestimates the effective core length^s of the bunch.

Summary

The resistive part of the VUV-ring longitudinal coupling impedance seems to be of the order of $(Z_{||}/n)_{res}^{WWR} \sim 10-12$ ohms and the reactive part of the order of $(Z_{||}/n)_{react}^0 \approx 4-5$ ohms. For an ideal $Q=1$ Broadband impedance of the resonant type, these two values should be comparable. The inconsistency could be accounted for by a ceramic element inside the beam chamber which absorbs heat from the beam, and adds a constant resistance to the system. This has to be further pursued.

The bunch lengthening as a function of beam current, although not ideally behaving like a pure microwave blow-up theoretical prediction, is not totally inconsistent with it.

The dipole mode transfer function should be remeasured by phase modulating the RF if possible.

The rather pathological behavior of the beam response beyond a current of about 30 mA in a single bunch ~~should~~ ~~be~~ needs further looking into.

One could adjust the sextupoles so as to give a negative chromaticity to the ring. Observation of the head-tail growth rate and head-tail transverse coherent frequency as a function of beam current will give us estimates of the transverse impedance.

VUV main parameters

$$C = 2\pi R = 51 \text{ m.}$$

$$\alpha = \text{Mom. Comp} = -0.23$$

$$\eta = -\frac{1}{\gamma_{tr}^2} + \alpha \approx .023$$

$$f_c = \text{Beam pipe cutoff} = 1.8 \text{ GHz.}$$

$$h = \text{RF harmonic} = 9.$$

$$f_0 \approx 5.876 \text{ MHz}$$

$$f_{RF} = 52.88525 \text{ MHz.}$$

$$f_s = 8.215 \text{ kHz @ } V_{RF} = 45.5 \text{ kV.}$$

Refs:

1. A. Hofmann and T. Risselada, IEEE Trans. Nucl. Sci., NS-30, 2400 (1983).
2. P. Wilson, J. Styles and K. Bone, IEEE Trans. Nucl. Sci., NS-24, 1496 (1977).
3. J. L. Laclare, "Bunched Beam Instabilities", Proc. Int. Conf. on Part. Accelerators, Geneva, July, 1980.
4. S. Hansen, et al. IEEE Trans. Nucl. Sci., Vol. NS-22, No. 3, June 1975.
5. G. Besnier, Nucl. Instr. Methods 164 (1979), pp 234-245.